

AD-A036 350

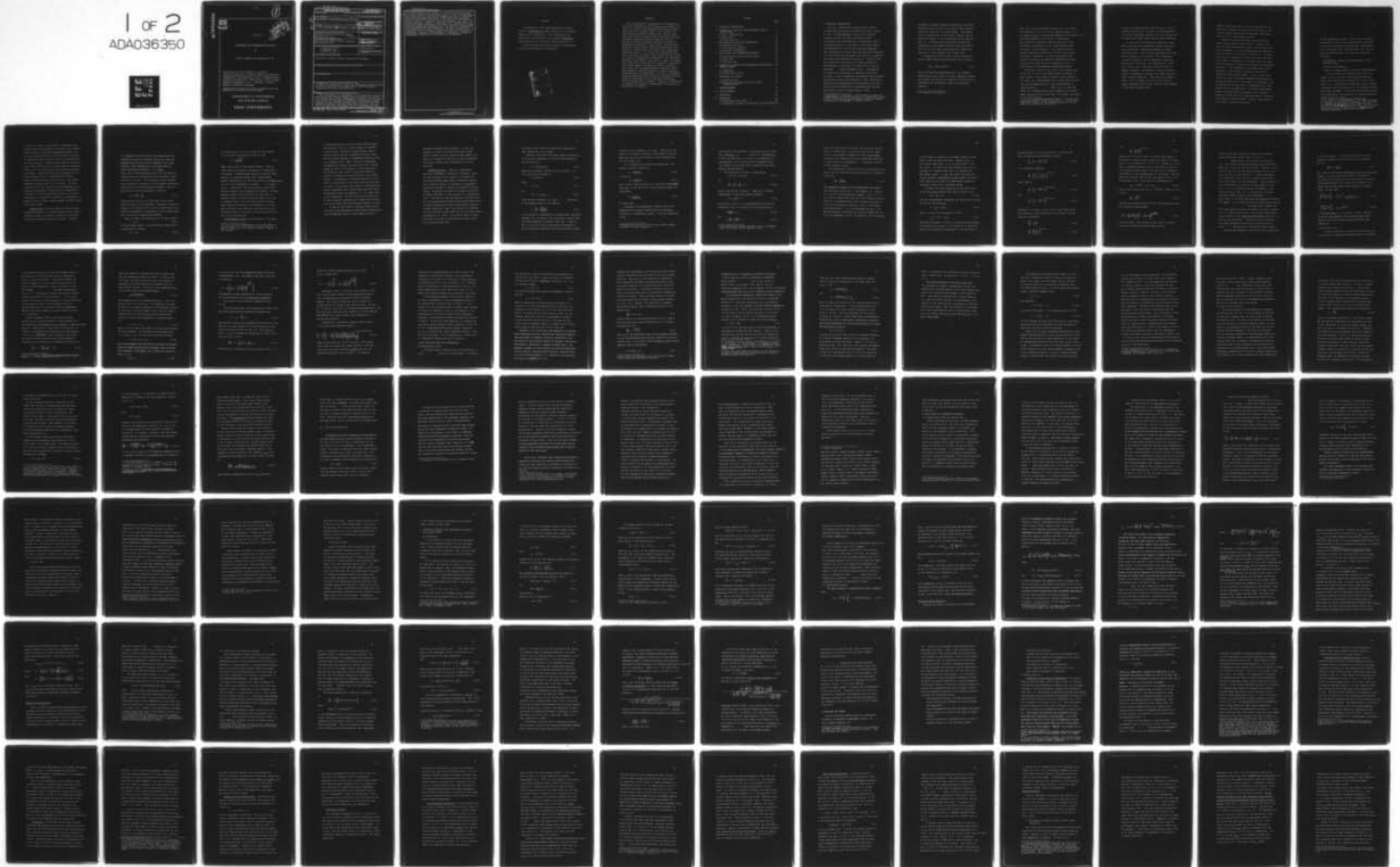
YALE UNIV NEW HAVEN CONN DEPT OF ENGINEERING AND AP--ETC F/G 20/4
GASDYNAMICS AND HOMOGENEOUS NUCLEATION, (U)
JUN 75 P P WEGENER, B J WU

N00014-67-A-0097-0012
NL

UNCLASSIFIED

31

1 of 2
ADA036350



ADA 036350



1

June 1975

D D C
R R R R R
MAR 3 1977
C

GASDYNAMICS AND HOMOGENEOUS NUCLEATION

by

Peter P. Wegener and Benjamin J.C. Wu

Distribution of this document is unlimited.

Report #31 prepared for Contract N00014-67-A-0097-0012:
"Experimental and Theoretical Study of Condensation by
Homogeneous Nucleation", (Power Branch, Office of Naval
Research, Washington, D.C.). Submitted by Peter P.
Wegener, Principal Investigator

Reproduction in whole or in part is permitted for any
purpose of the United States Government.

DEPARTMENT OF ENGINEERING
AND APPLIED SCIENCE
YALE UNIVERSITY

Unclassified

SECURITY CLASSIFICATION OF THIS PAGE (When Data Entered)

REPORT DOCUMENTATION PAGE		READ INSTRUCTIONS BEFORE COMPLETING FORM
1. REPORT NUMBER	2. GOVT ACCESSION NO.	3. RECIPIENT'S CATALOG NUMBER
4. TITLE (and Subtitle) GASDYNAMICS AND HOMOGENEOUS NUCLEATION		5. TYPE OF REPORT & PERIOD COVERED
7. AUTHOR(s) Peter P./Wegener Benjamin J.C./Wu		6. PERFORMING ORG. REPORT NUMBER 15 14 31
9. PERFORMING ORGANIZATION NAME AND ADDRESS Department of Engineering and Applied Yale University Science New Haven, CT. 06520		8. CONTRACT OR GRANT NUMBER(s) N00014-67-A-0097-0012
11. CONTROLLING OFFICE NAME AND ADDRESS Power Program, Office of Naval Research Arlington, VA 22217		10. PROGRAM ELEMENT, PROJECT, TASK AREA & WORK UNIT NUMBERS
14. MONITORING AGENCY NAME & ADDRESS (if different from Controlling Office) 12 139p.		12. REPORT DATE June 1975
16. DISTRIBUTION STATEMENT (of this Report) Approved for public release, distribution unlimited.		13. NUMBER OF PAGES 84
17. DISTRIBUTION STATEMENT (of the abstract entered in Block 20, if different from Report)		15. SECURITY CLASS. (of this report) Unclassified
18. SUPPLEMENTARY NOTES		15a. DECLASSIFICATION/DOWNGRADING SCHEDULE
19. KEY WORDS (Continue on reverse side if necessary and identify by block number) Condensation, Nucleation, Clustering, Measurement, Flow, Nozzles, Gas Flow, Expansion, Shock Tubes, Drops, Growth (General), Evaporation, Gas Flow, and Molecules.		
20. ABSTRACT (Continue on reverse side if necessary and identify by block number) The fundamentals of gasdynamics of one-dimensional flows with condensation are reviewed paying special attention to concepts from nonequilibrium flows, homogeneous nucleation, droplet growth. Flow systems for experimental research in condensation, namely steady-flow Laval nozzles, Ludwig tubes, shock tubes and high intensity supersonic molecular beams are discussed. New and previously published experimental results on homogeneous nucle- ation of eight vapors, obtained using gasdynamic methods, were		

DD FORM 1473 1 JAN 73 EDITION OF 1 NOV 65 IS OBSOLETE

Unclassified 400 987
SECURITY CLASSIFICATION OF THIS PAGE (When Data Entered)

Unclassified

SECURITY CLASSIFICATION OF THIS PAGE(When Data Entered)

critically examined and compared on a uniform basis with steady state homogeneous nucleation theory. It is found that experiments with water, nitrogen and ethanol vapors agree with the classical theory of homogeneous nucleation or the statistical mechanics theory based on the models of Kuhrt and Dunning. This study also revealed that in a number of experiments with several vapors, in which much higher nucleation rates than those calculated from the classical theory were thought to have been observed, involve ambiguous interpretations and assumptions. To date, no experiment using any method has shown conclusive agreement with the Lothe and Pound model of the statistical mechanical theory of homogeneous nucleation. Finally, a bibliography of condensation studies in compressible flow systems is provided in the appendix.

Unclassified

SECURITY CLASSIFICATION OF THIS PAGE(When Data Entered)

Foreword

The material in this report represents a contribution to Nucleation II, Marcel Dekker, N.Y. (in press), edited by A.C. Zettlemoyer. This contribution was solicited by the editor who also assembled Nucleation, Marcel Dekker, N.Y., 1969 (now called "Nucleation I").

Since the material includes original contributions, it is first published as an ONR Report.

ADDRESS	DATE RECEIVED	<input checked="" type="checkbox"/>
FROM	DATE FORWARDED	<input type="checkbox"/>
BY	SUBMITTED TO	
BY	DATE	
A		

ABSTRACT

The fundamentals of gasdynamics of one-dimensional flows with condensation are reviewed paying special attention to concepts from nonequilibrium flows, homogeneous nucleation, droplet growth. Flow systems for experimental research in condensation, namely steady-flow Laval nozzles, Ludwieg tubes, shock tubes and high intensity supersonic molecular beams are discussed. New and previously published experimental results on homogeneous nucleation of eight vapors, obtained using gasdynamic methods, were critically examined and compared on a uniform basis with steady state homogeneous nucleation theory. It is found that experiments with water, nitrogen and ethanol vapors agree with the classical theory of homogeneous nucleation or the statistical mechanics theory based on the models of Kuhrt or Dunning. This study also revealed that in a number of experiments with several vapors, in which much higher nucleation rates than those calculated from the classical theory were thought to have been observed, involved ambiguous interpretations and assumptions. To date, no experiment using any method has shown conclusive agreement with the Lothe and Pound model of the statistical mechanical theory of homogeneous nucleation. Finally, a bibliography of condensation studies in compressible flow systems is provided in the appendix.

OUTLINE

	Page
1 HISTORICAL INTRODUCTION.	1
2 COMPRESSIBLE, INVISCID, ONE-DIMENSIONAL FLOW OF PERFECT GASES.	6
a) Basic Considerations.	6
b) Nozzle Flow.	13
c) Shock Tube Flow.	20
3 REAL GASES AND FLOW WITH CONDENSATION.	25
a) Nonequilibrium Flow.	25
b) Flow with Heat Addition.	33
c) Flow with Condensation.	38
4 FLOW SYSTEMS FOR CONDENSATION RESEARCH.	44
a) Steady Nozzle Flow and Ludwig Tube.	44
b) Shock Tube.	49
c) Molecular Beam.	52
5 EQUATIONS OF MOTION WITH HOMOGENEOUS NUCLEATION AND DROPLET GROWTH.	53
a) Gasdynamics.	53
b) Condensation Kinetics.	57
6 EXPERIMENT AND THEORY.	71
a) General Results.	73
b) Experiment and Theory for the Critical Supersaturation	87
7 ACKNOWLEDGMENTS.	95
8 LIST OF SYMBOLS.	96
9 REFERENCES.	100
10 APPENDIXES.	107
1) Compressible Flow Table.	107
2) Condensation Studies in Compressible Flow Systems.	108

1 HISTORICAL INTRODUCTION.

The first international congress wholly devoted to high speed flight and gasdynamics* was held in Rome in 1935. At that meeting, Prandtl (1935) showed a schlieren picture of nozzle flow (Fig.1.1) and he pointed to the then-mysterious disturbances seen in the supersonic flow to the right of the nozzle throat. Wieselsberger** in the ensuing discussion suggested that condensation of water vapor may have been responsible for these shock-like phenomena since Prandtl's supersonic wind tunnel was operated with moist air. Shortly after the Rome meeting this guess was indeed confirmed at Wieselsberger's laboratory in Aachen with the results published later by Hermann (1942). Subsequently air driers were introduced in supersonic wind tunnel circuits to avoid condensation disturbances which rendered quantitative model tests impossible. Thus, condensation problems entered gasdynamics and aeronautics by an accidental discovery while water condensation has long ago been known to occur in steam nozzles. These

* Gasdynamics is the regime of fluid mechanics where the compressibility of the fluid needs to be taken into account.

** For a brief history of these early events and detailed references see the Appendix of Wegener (1975).

convergent-divergent nozzles introduced by the Swedish engineer de Laval in 1883 (e.g. Stodola 1927) produced supersonic steam flow in steam turbines. The appearance of condensation in such nozzles, however, was delayed with respect to the coexistence line as shown in Fig. 1.2. From many such observations an empirical condensation curve emerged which was named the "Wilson line" to honor the early investigator of delayed condensation in cloud chambers (e.g. Wilson 1897).

Condensation of water vapor in air in supersonic nozzles obeyed empirical relationships and a function

$$\Delta T_{ad} = f(\phi_o, dT/dt) , \quad (1.1)$$

could be established experimentally.* The adiabatic supercooling ΔT_{ad} is taken to be the temperature difference between the location of saturation and the onset of condensation on an adiabatic (here, an isentropic) expansion.

* For symbols note Section 8.

This term is also illustrated in Fig. 1.2. It is moreover apparent, that the "critical supersaturation", i.e. the ratio, p_{vk}/p_{∞} , of the partial pressure of the vapor to its saturation pressure at the onset of condensation is an equivalent method to describe the state of the spontaneous condensation in the supersaturated state. For $\Delta T_{ad} > 0$, we have $p_{vk}/p_{\infty} > 1$. In supersonic flow we normally experience high values of the critical supersaturation, therefore it is usually easier and more accurate to express the onset of condensation in terms of ΔT_{ad} since slight errors in temperature result in large errors in the tabulated saturation pressure.

The primary effect on the value of the supercooling in Eq.(1.1) is due to the initial partial pressure of water vapor, or the relative humidity in the supply of the nozzle, ϕ_0 . Experimental data on this effect in nozzle flow are shown in Fig. 1.3 at a cooling rate of about $10^5 C/sec$. Next, Fig. 1.4 shows the effect of a variable cooling rate observed in a Prandtl-Meyer expansion* with a functional relationship also shown

* Such an isentropic expansion arises in a steady supersonic flow around a sharp convex corner. It is the two-dimensional analog of the unsteady expansion in shock tubes to be discussed in Section 2c.

to admit the proper physical limit at $\Delta T_{ad} = 0$ for a vanishing cooling rate. We note, for this experiment as for other gasdynamic methods, that the cooling rates are appreciably higher than those of other techniques.

It took until 1940 before this empirical result and in fact the entire gasdynamic process were physically understood. Displaying remarkable insight, Oswatitsch (1941, 1942) provided experimental and theoretical evidence on the nature of the condensation process in supersonic flow (homogeneous nucleation, growth laws, time scales, heat addition, etc.) that still stands today. Moreover, he was the first to suggest supersonic flow methods to study condensation itself by proposing to measure the surface tension of small clusters indirectly. This task still eludes us today. Thus, he added a new tool to the chemical physics laboratory that rivals Wilson's cloud chamber in importance (Dunning 1960).

Finally, Oswatitsch noted the cross connection of condensation in supersonic wind tunnels with that in steam turbine nozzles and he employed identical theoretical methods for the understanding of both.

Gasdynamic methods have since been enlarged by adding shock tubes and other devices. However, they all have some common features which set them apart from other techniques. For one, heterogeneous nucleation on aerosols present in the flow is unimportant. The short time scales of supersonic flow are such that even maximized rates of condensation on foreign nuclei are negligible in relation to condensation produced by homogeneous nucleation. This situation is unchanged even in the presence of large numbers of aerosols, say $10^6/\text{cm}^3$, (Oswatitsch 1942, Wegener 1969). It is, in fact, difficult to affect the normally homogeneous nucleation by seeding the moist air in the supply of a supersonic nozzle (Buckle and Pouring 1965). Supersaturation is generally found to be high owing to the high cooling rates because the short time scale permits only a reduced number of collisions of the condensing vapor in relation, for example to a cloud chamber. However, these effects still permit a detailed resolution

of the condensation process. Rather than the single measurement of the critical supersaturation possible in Wilson and diffusion cloud chambers, condensation rate, nucleation rates, droplet growth, etc., may be measured quantitatively in a precisely prepared environment.

2 COMPRESSIBLE, INVISCID, ONE-DIMENSIONAL FLOW OF PERFECT GASES.*

a) Basic Considerations

Effects of compressibility arise in fluid mechanics if flow speeds exceed about one third of the speed of sound, and this technologically important regime has received much attention in the last forty years or so. The advent of supersonic flight, rocketry, atmospheric entry from space, etc. has moreover spurred much recent progress. In such flows, the density varies and in addition to the equations of motion, an equation

* This section is addressed to those who may not be familiar with gasdynamics. For details we refer to textbooks such as those by Liepmann, H.W. and Roshko, A., Elements of Gasdynamics, Wiley, New York 1957, Becker, E., Gas Dynamics, Academic Press, New York 1968, and Vincenti, W.G. and Kruger, C.H., Introduction to Physical Gasdynamics, Wiley, New York 1965.

of state, $p = p(\rho, T)$, is required. Conversely, gasdynamics had a strong impact on chemistry (e.g. Wegener 1966) since well understood gasdynamic processes such as shock waves provide tools for the study of reactions at controlled time resolutions that have traditionally not been available. Nonequilibrium flows are important (e.g. Becker 1972) where one or more modes of molecular motion, etc. of a gas mixture depart from thermodynamic equilibrium. Rapid condensation by homogeneous nucleation represents such a nonequilibrium situation. However, before studying real gas flows, a few simple gasdynamic concepts need to be clarified. This discussion will set the stage for an understanding of the particular advantages of high speed flow experiments in relation to the more traditional devices in the field. Gasdynamics is described in relation to condensation in greater detail by Stever (1958), Wegener and Mack (1958), and Wegener (1969).

Inviscid Flow: All shear flows, or flows in which neighboring layers of the fluid (liquid or gas) exhibit different speeds, are subject to laminar or turbulent exchange of momentum between these layers. However,

it is found in practice that at low shear rates, the internal friction (or turbulent motion) can often be neglected and the fluid can be treated as if it were inviscid. This idealization of the real fluid is never valid near solid walls. In a narrow layer, the so-called boundary layer, the flow speed is reduced from the undisturbed free stream speed to zero velocity at the wall. The structure of this boundary layer (laminar or turbulent), and its lateral extent are governed by the well-known Reynolds number. This dimensionless similarity parameter is given by

$$\text{Re} \equiv \frac{\rho u l}{\eta} = \frac{u l}{\nu} , \quad (2.1)$$

expressing the ratio of the inertial to the viscous forces acting on a fluid element. Generally at Reynolds numbers of the order of 10^4 to 10^6 as found in most condensation experiments in gasdynamics, the boundary layers near the walls of a nozzle are turbulent.

Next, we recall the definitions of the Mach number:

$$M \equiv u/a , \quad (2.2)$$

and the Knudsen number, relating the mean free path to a characteristic length:

$$\text{Kn} \equiv \lambda/l . \quad (2.3)$$

By combining Eqs. (2.1), (2.2) and (2.3) and making use of concepts from kinetic theory we find

$$\text{Kn} = \frac{M}{\text{Re}} \sqrt{\frac{4}{3}\gamma} \quad (2.4)$$

where γ is the ratio of the specific heats.* Here all three important similarity parameters of compressible flow appear. Excepting high intensity molecular beams produced by supersonic nozzle flow, large Knudsen numbers characteristic of the free molecule flow (FMF) regime are not found in gasdynamics research on condensation. Rather, $\text{Kn} \ll 1$ for the previously quoted high Reynolds numbers, and continuum flow prevails. At high Reynolds numbers, viscous effects are small and the boundary layers are found to be very narrow (e.g. Fig. 8, Wegener, 1969). For such nearly inviscid flows, a small empirical correction can be applied to the geometrical nozzle cross-sectional area resulting in an "effective area" to be used in the inviscid flow treatment to be discussed next.

One-dimensional Flow: The requirement of low shear

* It is customary in gasdynamics to use the symbol, γ , for this term. We shall therefore later denote the surface tension by σ , in contrast to other chapters in this volume.

to produce practically inviscid flows further demands flow systems of low or no wall curvature in addition to the previous criterion of high Reynolds numbers. Typical nozzles used for condensation studies, again with the marked exception of gasdynamic molecular beams (e.g. Anderson et al. 1966), consist of converging-diverging ducts having flat walls with total included angles of about 5 to 10 degrees. These plane walls are joined by cubic curves in the throat region to provide a continuous second derivative of the surface profile. Consequently, a uniform acceleration of the flow at the junctures of the cubic curve and the plane is found. In such ducts the concept of one-dimensional flow is applicable with a practically uniform velocity distribution across the channel, i.e. at a right angle to the streamlines. In fact if we have $A(x)$ given by a static pressure calibration of a nozzle (see Section 2b), we can later find $u(x)$ from the equation of motion.

In turn in shock tubes of constant cross section the flow is one-dimensional by definition provided again that the Reynolds number is high enough to insure a

negligible boundary layer thickness. In sum, the treatment of nozzle and shock tube flows at high Reynolds numbers and low supersonic Mach numbers will permit us to apply the equations of motion simplified for inviscid (ideal) and one-dimensional flow respectively.

Equation of State: Finally, a substantial analytical advantage is obtained if the gases, vapors and their mixtures can be treated as thermally and calorically perfect gases until condensation appears. This assumption applies in particular to gasdynamic experiments designed to study the condensation process itself. Exceptions are found for thermal non-ideality at higher pressures in steam nozzles (e.g. Barschdorff 1971). The need for real gas equations including those for the supersaturated states becomes particularly acute in modern high pressure steam turbines since states at extreme conditions of say 50 bar pressure at condensation are required to make efficient use of nuclear plants (Gyarmathy et al. 1973). On the other hand, in shock tube work, the study of condensation of metal vapors (e.g. Kung and Bauer 1971)

may require that caloric non-idealities appearing at high temperatures are included.

However, aside from these less frequent situations, the ideal gas assumption is valid and the equation of state is given by

$$p = RT \sum_j (\rho_j / \mu_j) , \quad (2.5)$$

where the subscript j denotes the j 'th species. Eq. (2.5) can also be written as

$$p = \rho(R/\mu)T , \quad (2.6)$$

where

$$\rho = \sum_i \rho_i , \quad (2.7)$$

and

$$1/\mu = \sum (\omega_j / \mu_j) , \quad (2.8)$$

using the mass fraction, $\omega_j = \rho_j / \rho$. The ratio of the specific heats, γ , is given by

$$\gamma = \frac{c_p}{c_v} = \frac{\sum_j \omega_j c_{pj}}{\sum_j \omega_j c_{vj}} . \quad (2.9)$$

It is practical in gasdynamics to express heat capacities, enthalpy, etc. in terms of unit mass and to employ lower case letter symbols to designate this fact. Finally, Eqs. (2.5) and (2.6) can later readily be adapted to include partially condensed flow by introducing the mass

fraction of the condensate, $g \equiv \rho'_c / \rho_T$. Here, ρ'_c is the density of condensate referred to the volume of the gas phase and ρ_T is the total density of the two-phase medium (see Section 5a).

For a thermally and calorically perfect gas, the acoustic velocity, defined by:

$$a = \sqrt{(\partial p / \partial \rho)_s} \quad , \quad (2.10)$$

is given by

$$a = \sqrt{\gamma(R/\mu)T} \quad , \quad (2.11)$$

with γ and μ given by Eqs. (2.9) and (2.8) respectively. Using Eqs. (2.11) and (2.2), we have the Mach number for ideal gases:

$$M = \frac{u}{\sqrt{\gamma(R/\mu)T}} \quad . \quad (2.12)$$

b) Nozzle Flow.

Isentropic, one-dimensional, steady* nozzle flow exemplifies the special attractiveness of gasdynamic techniques in condensation studies. With the assumptions of the

* Steady flows are those in which no parameter changes with time at a given location.

last section, the equations to be derived for this flow will, moreover, be useful for a determination of the starting point, or "onset", of condensation in nozzles, since up to this point the condensation process cannot yet interfere with a supersonic flow. The results are as follows.*

The conservation of mass is expressed by:

$$\rho u A = \dot{Q} = \text{constant}, \quad (2.13)$$

or

$$\frac{d\rho}{\rho} + \frac{du}{u} + \frac{dA}{A} = 0. \quad (2.14)$$

Newton's second law of motion applied to a moving, compressible fluid yields Euler's equation

$$u \, du + \frac{dp}{\rho} = 0. \quad (2.15)$$

Similarly, for later use in one-dimensional flow in the x-direction, Eqs. (2.13) and (2.15) can be written as

$$\frac{d(\rho u A)}{dx} = 0, \quad (2.16)$$

and

$$u \frac{du}{dx} + \frac{1}{\rho} \frac{dp}{dx} = 0, \quad (2.17)$$

* For details note Wegener and Mack (1958), and Wegener (1969) in addition to the textbooks cited.

where the term $u(du/dx)$ expresses the convective acceleration in steady flow. We realize that while in steady flow no flow parameter changes with time, a gas sample undergoing the expansion alters its properties from point to point since it is convected to different locations having different states.

By combining Eqs. (2.6), (2.12), (2.14), and (2.15) we can derive the well-known area-velocity relation for compressible flow,

$$\frac{du}{u} = \frac{-dA/A}{1 - M^2} . \quad (2.18)$$

The fundamental equation for incompressible flow yields the well-known result $du/u = -dA/A$ since $M = 0$. However, if $M \neq 0$, the following pattern emerges. For $0 < M < 1$ (or subsonic speeds with $u < a$), Eq. (2.18) behaves qualitatively as in incompressible flow; a decrease in area results in an increase in velocity. For $M > 1$ (or supersonic speeds with $u > a$), the denominator of Eq. (2.18) becomes negative, resulting in a positive coefficient for dA on the righthand side of the equation. Now an increase

of flow speed is caused by an increase in area, in contrast to the low speed situation. Finally at $M = 1$, (or at sonic speed with $u = a$), we have $(1-M^2) = 0$ in Eq. (2.18). In steady flow this condition can only be realized at a "throat" where $dA/A = 0$, because du/u must remain finite. In sum, flow from a low speed reservoir through a converging-diverging nozzle can attain sonic speed at the throat and subsequently proceed to supersonic speeds in the diverging passage.

To obtain the local properties of the nozzle flow, we add the energy equation for steady adiabatic flow:

$$dh + udu = 0. \quad (2.19)$$

With the thermodynamic assumptions of the previous section we find for the enthalpy

$$h = c_p T + \text{const.}, \quad (2.20)$$

and Eq. (2.19) can be integrated to give

$$c_p T + u^2/2 = c_p T_o, \quad (2.21)$$

where the subscript, o , refers to the known nozzle supply or reservoir state where $u = 0$. Moreover, T_o may be defined as the stagnation temperature of the gas after it

has been brought to rest adiabatically. With the previous assumptions and definitions we find:

$$\frac{T}{T_0} = \left(1 + \frac{\gamma-1}{2} M^2 \right)^{-1} . \quad (2.22)$$

In an isentropic expansion:

$$\frac{P}{P_0} = \left(\frac{\rho}{\rho_0} \right)^\gamma = \left(\frac{T}{T_0} \right)^{\gamma/(\gamma-1)} , \quad (2.23)$$

which leads to:

$$\frac{P}{P_0} = \left(1 + \frac{\gamma-1}{2} M^2 \right)^{-\gamma/(\gamma-1)} , \quad (2.24)$$

and

$$\frac{\rho}{\rho_0} = \left(1 + \frac{\gamma-1}{2} M^2 \right)^{-1/(\gamma-1)} . \quad (2.25)$$

Setting $M = 1$, in Eqs. (2.22), (2.24), and (2.25) we get the critical or sonic conditions at the throat to be denoted by an asterisk:

$$\frac{T^*}{T_0} = \frac{2}{\gamma+1} , \quad (2.26)$$

$$\frac{P^*}{P_0} = \left(\frac{2}{\gamma+1} \right)^{\gamma/(\gamma-1)} , \quad (2.27)$$

and

$$\frac{\rho^*}{\rho_0} = \left(\frac{2}{\gamma+1} \right)^{1/(\gamma-1)} \quad (2.28)$$

Equation (2.27) tells us that to achieve sonic speed at the throat, a pressure ratio across the nozzle of at least $p_0/p^* = 1.9$ is needed for $\gamma = 7/5 = 1.4$. Indeed, Eq. (2.18) does not prohibit subsonic flow at the throat at insufficient pressure ratios across the nozzle with a subsequent deceleration in the diverging part of the nozzle. Moreover, should the pressure ratio exceed that given by Eq. (2.27), the constant in Eq. (2.13) can now be determined by:

$$\rho u A = \rho^* a^* A^* = \dot{Q} = \text{const.}, \quad (2.29)$$

from a fixed supply since $a^*/a_0 = (T^*/T_0)^{1/2}$. From Eq. (2.29) we find

$$\frac{A}{A^*} = \frac{\rho^* a^*}{\rho u}, \quad (2.30)$$

and from the formulas derived so far, the nozzle area ratio as a function of Mach number,

$$\frac{A}{A^*} = M \left[\left(\frac{\gamma+1}{2} \right) / \left(1 + \frac{\gamma-1}{2} M^2 \right) \right]^{\frac{\gamma+1}{2(\gamma-1)}}, \quad (2.31)$$

may be obtained. The function of Eq. (2.31) is double-valued and for each area ratio there are two

values of the Mach number for subsonic and supersonic speed respectively, while $A/A^* = 1$ at $M = 1$.

These results can now be put to practical use. For a given converging-diverging nozzle with known geometry, we have $A(x)$ and thus $A/A^*(x)$. From Eq. (2.31), we next find $M(x)$ and the previous formulas yield T/T_0 , p/p_0 , and ρ/ρ_0 at each location. A single measurement in a supersonic nozzle flow at a known location therefore fully defines all flow parameters. These parameters can be tabulated as a function of Mach number as given for $\gamma = 7/5 = 1.4$ (diatomic gases) in Appendix 1, and they are shown in Fig. 2.1. A rapid drop of pressure with Mach number is apparent and relatively high values of the supply pressure are required for the flow to remain in the continuum regime at higher Mach numbers.

For water vapor, ethanol and many other vapors, however, saturation is usually attained at $M < 1$, ahead of the throat. The delayed condensation occurs usually at low supersonic Mach numbers ($M < 1.5$), or shortly past the throat. Therefore even at relatively low supply pressures, free molecule flow does not yet enter. The geometry of the nozzle throat region controls the expansion rate and thus the cooling rate

of the vapor sample. In steady nozzle flow such time dependent variables can be found from the local gradients by

$$\frac{d(\quad)}{dt} = u \frac{d(\quad)}{dx}, \quad (2.32)$$

where any of the derived parameters may be put in the parentheses. For a two-dimensional nozzle, the change of area ratio with distance in the throat region can be related geometrically to the radius of curvature of the throat, R^* , and the nozzle throat height, h^* (Wegener 1964). We then find

$$\left[\frac{d(T/T_o)}{dt} \right]^* = - (R^* h^*)^{-\frac{1}{2}} \frac{\gamma-1}{[(\gamma+1)/2]^2} a_o, \quad (2.33)$$

or

$$\left[\frac{d(T/T_o)}{dt} \right]^* = - C a_o (R^* h^*)^{-\frac{1}{2}}. \quad (2.34)$$

For diatomic gases, $\gamma = 7/5$, and $C = 0.278$. From Eq. (2.34) we find remarkably high cooling rates of the order of 10^6 C/sec for small research nozzles (See Section 6).

c) Shock Tube Flow

A simple shock tube is a duct of uniform cross section in which a removable diaphragm divides two chambers.

In these chambers there are carefully prepared gases or gas mixtures at different pressures and temperatures prior to a given experiment. These gases undergo controlled changes in a wave system resulting from the rupture of the diaphragm to equalize conditions in the two chambers as shown schematically in Fig. 2.2. Condensation research has utilized several different sections of the wave system to be described in Section 4b. The gasdynamics of shock tube flows is discussed in detail in the textbooks cited and special applications to physical chemistry exploiting the well controlled changes in the gas sample are given e.g. by Bradley.*

After diaphragm rupture a shock wave develops rapidly and this wave proceeds at a uniform speed into the undisturbed low pressure gas at condition 1. The shock Mach number is defined by $M_s = u_s/a_1$ where the subscript, s, relates to the speed of the shock wave. We have from Eq. (2.11), $a_1 = \sqrt{\gamma_1(R/\mu_1)T_1}$, and the pressure jump across the wave is given by the well-known Rankine-Hugoniot relation for a calorically and thermally perfect gas by:

$$\frac{P_2}{P_1} = 1 + \frac{2\gamma_1}{\gamma_1+1} (M_s^2 - 1) , \quad (2.35)$$

* John N. Bradley, "Shock Waves in Chemistry and Physics," Methuen Co., London, Wiley, N.Y. 1962.

where the subscript 2 denotes the state at higher pressure and temperature behind the shock. As seen in Fig. 2.2, $p_4 > p_1$, and while the shock moves to the right, an isentropic, unsteady expansion fan proceeds into the high pressure chamber. The front of this expansion moves at the sound speed of the medium ahead:

$$a_4 = \sqrt{\gamma_4 (R/\mu_4) T_4} , \quad (2.36)$$

where again as in all following equations, γ and μ are given by Eqs. (2.8) and (2.9). The expansion fan shown in Fig. 2.2 is ideally centered at the diaphragm location at time zero, and each straight line in the fan, being a characteristic of the governing partial differential equation, defines wave propagation at constant speed, c , by

$$c = x/t = u - a. \quad (2.37)$$

Here, u , is the local flow speed of the gas moving towards the lower pressure. At the head of the expansion fan, $u = 0$, and $c = a_4$. At the tail of the same fan where

$$c_3 = x/t = u_3 - a_3 , \quad (2.38)$$

the outflow speed of the gas initially located in the high pressure chamber may be locally subsonic, sonic or supersonic depending on the slope (x/t) of the last characteristic c_3 , i.e.

$$a_3 \begin{matrix} > \\ < \end{matrix} u_3 . \quad (2.39)$$

It can be shown that the propagation speed of this last characteristic, i.e., the speed of the tail of the fan is given by:

$$c_3 = a_4 \left[\frac{2}{\gamma_4 - 1} - \frac{\gamma_4 + 1}{\gamma_4 - 1} \left(\frac{p_3}{p_4} \right)^{\frac{\gamma_4 - 1}{2\gamma_4}} \right]. \quad (2.40)$$

The pressure on each characteristic in the expansion fan may be related to the corresponding temperature and density in the isentropic expansion by Eq. (2.23).

The local wave speed can be expressed in terms of the local flow speed and the conditions in region 4 by:

$$c = -a_4 + \frac{\gamma_4 + 1}{2} u. \quad (2.41)$$

This equation allows us to determine the path of an actual particle (or small volume) of the flow starting at some initial location as shown in Fig. 2.2. This particle path $x = x(t)$ is obtained by integrating the local fluid velocity in Eq. (2.41):

$$\frac{dx}{dt} \equiv u = \frac{2}{\gamma_4 + 1} \frac{x}{t} + \frac{2}{\gamma_4 + 1} a_4. \quad (2.42)$$

The history of a particle can now be traced in the $x - t$

plane with initial particle position, x_0 at time t_0 ($t_0 = x_0/a_4$), by:

$$x(t) = -\frac{a_4 t}{\gamma_4 - 1} \left[2 - (\gamma_4 + 1) \left(\frac{t_0}{t} \right)^{\frac{\gamma_4 - 1}{\gamma_4 + 1}} \right]. \quad (2.43)$$

Returning to Fig. 2.2 we note a last feature of the flow, the so-called contact surface separating states 2 and 3 corresponding to the gases initially in either chamber. The contact surface may also be viewed as a virtual piston set abruptly into uniform motion. We find $u_2 = u_3$ and $p_2 = p_3$, but $T_3 < T_2$ since the expanded gas on the left has been cooled while the shocked gas on the right has been heated. The contact surface thus represents an entropy discontinuity.

Combining the conservation laws, we finally arrive at the shock tube operating equation

$$\frac{p_4}{p_1} = \frac{p_2}{p_1} \left\{ 1 - \frac{(\gamma_4 - 1)(a_1/a_4)[(p_2/p_1) - 1]}{\sqrt{2\gamma_1} \sqrt{2\gamma_1 + (\gamma_1 + 1)} [(p_2/p_1) - 1]} \right\}^{-(2\gamma_4)/(\gamma_4 - 1)}, \quad (2.44)$$

where we can insert Eq. (2.35) for p_2/p_1 . This substitution links the shock Mach number directly to the initial conditions that are known a priori and thus the remaining parameters can be computed. The maximum

expansion and correspondingly the lowest pressure and temperature respectively achieved in the isentropic, unsteady fan is found e.g., from $p_3/p_4 = (p_2/p_1)/(p_4/p_1)$ in conjunction with Eq. (2.44) since $p_3 = p_2$. Instantaneous distributions of these properties at time t_1 , are shown schematically in the lower part of Fig. 2.2 together with symbols denoting the conditions in the tube.

At high Reynolds numbers, small viscous effects or the minor consequences of finite diaphragm rupture can be accounted for as will be seen in Section 4. The reasons for this fortunate state of affairs were outlined in Section 2a. However, a check of the ideality of the tube operation is usually provided by the redundancy inherent in the measured variables entering the equations of motion. Usually the shock speed, u_s , is measured and thus p_2/p_1 can be computed directly from Eqs. (2.12) and (2.35). Independently, with known initial conditions, $p_3 = p_2$ is measured and overall agreement with Eq. (2.44) can thus be checked. For the application of these flows to condensation studies, we refer to Section 4.

3 REAL GASES AND FLOW WITH CONDENSATION

a) Nonequilibrium Flow

In certain flows, the behavior of real gases may deviate from that of ideal gases. In terms of

the equation of state, such deviations may generally be divided into two classes: those resulting in an equation of state involving two independent variables, e.g., for the internal energy,

$$e = e(\rho, s), \quad (3.1)$$

and those requiring more than two independent variables, such as

$$e = e(\rho, s, \phi). \quad (3.2)$$

Here the additional so-called progress variable, ϕ , is required to fix the thermodynamic state of the gas. Non-idealities of the kind of Eq. (3.1) have been discussed before in conjunction with high pressure steam. No conceptual difficulty arises in the gasdynamic treatment of the flow since the function, Eq. (3.1), may be given in the form of diagrams, tables, or simply in more complicated equations than the ones for the ideal gas.

Equation (3.2) on the other hand applies to situations where departures from the thermodynamic equilibrium appear. This may happen if chemical reactions, excitation or de-excitation of some internal degrees of freedom of molecules, dissociation, ionization or changes of phase occur. The progress variable, ϕ , must therefore be defined differently in each specific non-equilibrium situation. When the flow is in the continuum regime, i.e., when $Kn \ll 1$, the gas molecules may be considered to be in

translational equilibrium, and the pressure and a "translational temperature" may be defined for the gas without ambiguity. Moreover, at the conditions of interest in most condensation problems the rotational mode of molecules may be taken to be in equilibrium and vibrational modes* are unexcited. Fortunately therefore, only one active relaxation mode needs be considered in homogeneous nucleation problems. Thus, the mass fraction of condensate may conveniently be taken as the progress variable, ϕ , in Eq. (3.2). However, the formalism of a general rate process applies, and a relaxation equation of the general form:

$$\frac{d\phi}{dt} = \Psi(\rho, s, \phi) , \quad (3.3)$$

arises, where Ψ is a prescribed function of ρ , s , and ϕ . For small deviations from equilibrium, Eq. (3.3) may be linearized to give

$$\frac{d\phi}{dt} = - \frac{(\phi - \phi_e)}{\tau} . \quad (3.4)$$

Here, ϕ_e is the equilibrium value of the progress variable ϕ (e.g. the condensate mass fraction) under the local conditions, and $\tau = \tau(\rho, s, \phi) > 0$ is the relaxation time with the property that at equilibrium,

$$\tau(\rho, s, \phi_e) = 0. \quad (3.5)$$

* This latter mode may have to be considered in condensation studies of polyatomic molecules.

Interesting work in gasdynamics concerns the behavior of these equations and it is discussed in different recent books.* More recent reviews by Marble (1969) on two-phase flows, Becker (1972) on chemically reacting flows, and by Wegener (1975) on condensing nonequilibrium flows are also of interest in this connection.

One additional fundamental problem that arises is the proper definition of the speed of sound in a condensing medium.** In a non-reacting medium, small disturbances propagate at the local acoustic velocity defined unambiguously by Eq. (2.10). Here, the differential in Eq. (2.10) is well defined since p may be expressed as a function of ρ and s using Eq. (3.1). In a condensing mixture, however, p is a function of three (or more) variables,

$$p = p(\rho, s, \phi), \quad (3.6)$$

as in Eq. (3.2), and thus there is an infinite number of differentials having the form $(\partial p / \partial \rho)_s$. Indeed in condensing flows we deal with the acoustics of dispersive media in treating the propagation of small disturbances.

* In addition to books cited at the beginning of Section 2, see Clarke, J.F. and McChesney, M., Dynamics of Real Gases, Butterworth, London (1964), and Wegener, P.P. (Ed.) Nonequilibrium Flows Parts I and II, Marcel Dekker, N.Y. (1969, 1970).

** Again the term condensing medium is to be interpreted broadly to include systems involving chemical reaction and other finite rate processes.

There are two limits with important physical significance in taking the derivative of the right hand side of Eq. (3.6):

$$a_f = \sqrt{(\partial p / \partial \rho)_{s, \phi}}, \quad (3.7)$$

and

$$a_e = \sqrt{(\partial p / \partial \rho)_{s, \phi = \phi_e}}. \quad (3.8)$$

Here, a_f and a_e are defined as the frozen and equilibrium sound speeds, respectively. The differentiation in Eq. (3.7) is taken with ϕ held constant regardless of the state of the gas. Thus the composition of the mixture is fixed, or "frozen". On the other hand, the differentiation in Eq. (3.8) is taken with ϕ retaining its equilibrium value appropriate for the prevailing state of the gas. The equilibrium condition

$$\phi_e = \phi_e(\rho, s), \quad (3.9)$$

is given by the law of mass action for chemical reactions, the Clausius-Clapeyron equation for condensation, or equivalents for other processes. When Eq. (3.9) is introduced in Eqs. (3.6) and (3.8), the classical gasdynamic result, Eq. (2.10) is recovered as expected. The terms "frozen" and "equilibrium" may, in turn, be interpreted to indicate the limiting behavior of the flow when the

rates of condensation are infinitely slow and infinitely rapid, respectively. We then have $\tau = \infty$ or $\tau = 0$ in Eq. (3.4).

Chu (1958) and Broer (1951) both showed that the characteristic speed of propagation of small disturbances in a reacting medium is the local frozen sound speed in all reacting flows having a finite reaction rate. Only when the reaction rate is truly infinite, i.e., when the flow is exactly in thermodynamics equilibrium, is the characteristic speed given by the equilibrium sound speed. Thus, the variation of characteristic speed with reaction rate is discontinuous, being a_f at all finite rates and a_e only when the rate is infinite (Chu 1958).

The definition of characteristic speed in a reacting flow is important because it serves to define the proper sound speed, the Mach number, and the direction of characteristics for the partial differential equations describing the flow. It can be shown using thermodynamic stability arguments that

$$a_f > a_e , \quad (3.10)$$

and typically

$$1.0 < a_f/a_e < 1.2 \quad (3.11)$$

for dissociating gases. For condensing flows we find:

$$1.1 < a_f/a_e < 1.8 \quad (3.12)$$

for H_2O (Wegener and Mack 1958) resulting in a much more pronounced effect of condensation on the dispersion of sound than the effect found in reactions.

Nozzle flow of gases undergoing dissociation or other single chemical reactions is well understood at this time. When the flow starts at a high temperature in the supply in thermodynamic equilibrium the gas may be partly dissociated. Recombination sets in as the gas mixture is cooled in the expansion. At some point determined largely by the local collision frequency of the gas, "sudden freezing" occurs as predicted by Bray (1959), the reaction ceases

and the flow departs from equilibrium. An interesting parallel may be drawn for nozzle flows with condensation (Wegener 1975).* In vapor expansions condensation is initially absent in the nozzle although the vapor may be highly supersaturated and the mixture composition remains constant. Hence in contrast to dissociating flow the expansion starts in the "frozen" condition. With the onset of condensation by nucleation and droplet growth saturation is attained quickly resulting in rapid vapor depletion. Henceforth the remaining vapor in the gas phase in the flow stays in equilibrium with the finely dispersed liquid phase. Thus condensation occurs spontaneously by "sudden equilibrium" in an exactly opposite process to that of "sudden freezing" discussed above for reacting flow. Analytical work has recently been done by Petty et al. (1972) in an attempt to locate the "sudden equilibrium" onset point of condensation through some simple criteria in the spirit of Bray's work.

In sum, we note that much experimental and theoretical work has been done on nonequilibrium nozzle flows and recent advances in the field have

* This suggestion was made by Prof. N.H. Johannesen of Manchester University in a discussion of an earlier paper by Wegener and Parlange (1967) on p. 633.

been reviewed by Bray (1970). Steady, shockless flows in slender nozzles involving a single nonequilibrium process are well understood at this time. This knowledge has been successfully used in recent years to determine the rate constants of some chemical processes through gasdynamic measurements of the nozzle flow and also to determine the rate of condensation by homogeneous and binary nucleation and cluster growth.

b) Flow with Heat Addition

The energy equation for one-dimensional, adiabatic and frictionless flow, Eq. (2.19) may easily be modified to admit heat exchange with the surroundings resulting in "diabatic flow." We shall not presently be concerned with the kinetics of this heat transfer; rather, we shall focus on the gasdynamic effects on the flow once the heat transfer has been completed. This view is consistent with our previous assumption of high Reynolds number flow with thin boundary layers. In compressible flow of real fluids, there will, in general, be temperature gradients along and normal to the streamlines, as dictated by the conditions at the flow boundary (e.g., heat conducting or insulating sidewalls held at fixed or variable temperature). Like velocity, it is found experimentally that temperature

variations across the streamlines are also restricted to a narrow region near the wall. In fact, a thermal boundary layer exists near the wall. Outside this layer the heat conductivity of the fluid plays no role, and the fluid behaves as though it were nonconducting. The ratio of the thickness of the thermal and the viscous boundary layers respectively is proportional to the inverse square root of the so-called Prandtl number. This dimensionless parameter is defined by:

$$\text{Pr} = \frac{nc_p}{\kappa}, \quad (3.13)$$

with κ , the thermal conductivity. The Prandtl number has the physical significance of expressing the ratio of the diffusivity of viscous to thermal effects respectively and for most gases we find $\text{Pr} \approx 1$. Therefore, the thermal and viscous boundary layers are roughly of the same thickness. In fact, in the one-dimensional treatment of nozzle flows using the effective area distribution given by a static pressure calibration discussed previously, both the viscous and the thermal boundary layers are accounted for, and the flow may be treated as inviscid and nonconducting. Within the boundary layer, the temperature increases from that given by the isentropic relation Eq. (2.22) roughly to

the stagnation temperature, T_0 , at the wall for those gases with $Pr \approx 1$.

In the following discussion, therefore, we can assume that the gas is nonconducting, and heat addition in one-dimensional flow is uniform at a given cross section normal to the flow direction. The amount of heat added to unit mass of the flow, q may, of course, vary with x and the function $q(x)$ depends on the process at hand. Heat addition of this kind is realized in flows subject to thermal radiation, flows with chemical reaction* (e.g. combustion), flows with condensation*, etc.

In the diabatic flows discussed, the continuity, momentum and thermodynamic state equations, (2.14), (2.15), and (2.16), remain valid. The energy equation, Eq. (2.19), for steady, adiabatic flow of an inviscid gas must now be modified by including a term dq to admit external heat exchange,

$$dh + u du = dq. \quad (3.14)$$

* It may be argued that in these cases no heat addition from an external source takes place. Heat is merely being transformed from one form to another. However, it is often more convenient and informative to consider flows with chemical reactions or condensation external heat-addition problems by a suitable choice of the system.

For an ideal gas, it is convenient to regard the heat addition as a change in the local stagnation temperature,* i.e.,

$$c_p dT + u du = c_p dT_o, \quad (3.15)$$

with

$$dq = c_p dT_o. \quad (3.16)$$

Detailed discussions of the influences of various processes on the gasdynamics variables, M , u , p , ρ , etc., of one-dimensional flow are available in Shapiro's textbook.** For example, in diabatic flow the changes in Mach number, cross-sectional area, and stagnation temperature are related by

$$\frac{dM^2}{M^2} = - \frac{2(1 + \frac{\gamma-1}{2}M^2)}{1-M^2} \frac{dA}{A} + \frac{(1+\gamma M^2)(1 + \frac{\gamma-1}{2}M^2)}{1-M^2} \frac{dT_o}{T_o}. \quad (3.17)$$

It can be seen from Eq. (3.17) that heat addition ($dT_o > 0$) to subsonic flow ($M < 1$) is accompanied by an increase in

* With heat addition, $T_o \neq T_{o1}$, where T_{o1} is e.g. the temperature in the supply of a nozzle. Often the subscript 1 is dropped, however.

** Shapiro, A.H., The Dynamics and Thermodynamics of Compressible Fluid Flow, Vols. I and II, Ronald Press, N.Y. (1953).

Mach number, while that to supersonic flow ($M > 1$) decreases the Mach number. Thus, heat addition always tends to drive the flow Mach number towards unity. Moreover, since the coefficients for dA and dT_0 in Eq. (3.17) are of opposite sign, the effects of heat addition on M are equivalent to and may be duplicated by an area reduction. This qualitative analogy between heat addition and area reduction is found to be generally valid for the influence on the other flow variables as well.

Using the area reduction analogy to heat addition we note that for a given Mach number there is a specific amount of heat that may be added to the gas stream which is equivalent to a reduction of the cross-sectional area to the critical throat area A^* . The Mach number after this critical heat addition will then be unity and at this point the flow becomes "thermally choked". This maximum or critical amount of heat addition, q_{\max} , (for condensation note Lukasiewicz and Royle 1948), is given by

$$\frac{q_{\max}}{c_p T_0} = \frac{(M^2 - 1)^2}{M^2 (\gamma^2 - 1) [M^2 + 2/(\gamma - 1)]} \quad (3.18)$$

Heat addition exceeding the value of q_{\max} may cause

shock waves or unsteady flows to occur (e.g. Wegener 1975), and these phenomena invalidate the simple treatment of Section 2. In this work, we shall only be interested in diabatic flow where the heat addition does not lead to thermal choking or discontinuities in the flow. Therefore, the basic conservation equations in the form of Eqs. (2.14), (2.15) and (3.14) remain valid.

3c. Flow with Condensation

Condensing flows show simultaneous nonequilibrium and heat addition effects and the progress variable ϕ for Eqs. (3.2) and (3.6) may be identified with the mass fraction g of the condensate. The thermodynamic state of the flow is fixed once g and two other thermodynamic variables, say p and T , are specified. The incremental heat addition per unit mass of mixture of the flow is related to the condensate mass fraction by:

$$dq = L_{\infty} dg. \quad (3.19)$$

Here, L_{∞} stands for the latent heat of the bulk condensate and possible curvature effects on this value (Wegener and Parlange 1967) are not considered.

Provided that the pressure ratio across the nozzle is sufficient to produce sonic flow at the nozzle throat, and that supercritical heat addition does not take place, integration of the gasdynamic equations for supersonic nozzle flows are rather straightforward.

The theory of supersonic nozzle flow with vapor condensation was first developed by Oswatitsch (1942). He showed that the presence, in the flow, of condensate droplets produced by homogeneous nucleation does not invalidate the assumption of inviscid flow because they are usually extremely small (typically $r \lesssim 1000\text{\AA}$) and thus they move practically with the gas stream.* Hence, the viscous drag between the droplets and the gas stream may be neglected outside the region of extreme

* For proof of this statement see e.g. Wegener (1969).

velocity gradients as found in shock waves or boundary layers. It may be argued that although the momentum transport between the gas stream and the droplets is negligible, the heat transfer across the phase boundary may not be ignored, and heat conduction ought to be included in the energy equation. In fact, it is due to the transfer of latent heat of condensation from the droplets to the gas phase that condensation is "felt" gasdynamically. However, since the condensate is found to be finely dispersed ($\sim 10^{12}/\text{cm}^3$) and therefore the droplets may be considered as uniformly distributed heat sources throughout the gas stream. Thus, the heat may be viewed as being generated internally in the gas phase and the problem of heat transfer between phases may be circumvented for the time being.*

Oswatitsch's assumption that condensation proceeds by homogeneous nucleation and droplet growth enabled him to compute the mass fraction of condensate as a function of the position along the nozzle by summing up the mass of all droplets

* On a different length scale, for example, in distances on the order of the diameter of the droplet, this heat transfer process may be important. In fact it is one limiting factor of the droplet growth rate.

present. He realized that although droplets of different sizes would be present at any given location along the nozzle, it was possible to determine the size of each individual droplet by tracing its history back to its origin as a nucleus of critical size and by integrating the growth rate along the particle path. Furthermore, he assumed that no disintegration or coalescence of droplets occurs resulting in the conservation of the number of droplets. Thus, both the total number of droplets and the size of each may be determined yielding the mass fraction of condensate. A condensation rate equation, in the general form of Eq. (3.3) may therefore be derived from a known droplet growth rate and nucleation rate. For this purpose, Oswatitsch (1942) gave a droplet growth equation, and he used the steady state homogeneous nucleation rate equation of Becker and Döring (1935) to describe the kinetics of condensation. The droplet growth law was based on an approximate free-molecule treatment of the simultaneous heat and mass transfer occurring at the surface of the droplet. For this assumption to be valid, the droplet diameter must be much smaller than the mean free path of

the surrounding gas, a condition satisfied in flows of vapor in the presence of an inert carrier gas. Typically for moist air, where the maximum droplet radii are about 100 \AA at the completion of condensation and the mean free path is of the order of 1000 \AA , Eq. (2.3) shows $Kn \sim 10$. For condensation of a pure vapor (e.g., steam), the droplets in the condensation zone eventually grow beyond 1000 \AA . However, in the region immediately downstream of the location where the droplets are formed, they are again of a sufficiently small size for the free molecule flow assumption to hold.

Under these assumptions, the primary effect of condensation on the supersonic nozzle flow is the addition of the latent heat of condensation to the gas stream. Therefore, the gasdynamic equations of motion are similar to those of one-dimensional, frictionless, diabatic, and steady flow, discussed before. If condensation occurs only in the supersonic section of the nozzle, integration in the flow direction may conveniently start at the throat, using the sonic conditions as a starting point. This situation avoids integration through the nozzle throat, which is a mathematical singularity as noted in the cited textbooks.

Thus, Oswatitsch was able to perform a stepwise numerical integration of the system of equations for steady

supersonic nozzle flow. In the pre-computer days of 1942 he obtained remarkable agreement of the theory with steam experiments (Yellot and Holland (1937), Binnie and Woods (1938)), and his own experiments with moist air. In the intervening years, Oswatitsch's formulation was consistently proven to be successful as adapted by many later investigators. Moreover, Oswatitsch's model has conversely become the basis for using supersonic nozzles in the experimental study of condensation phenomena.*

Along similar lines, one of us (B.J.C. Wu) has derived equations for the one-dimensional unsteady expansions

* Papers using this

approach include Wegener and Mack (1958), Stever (1958), Pouring (1963), Hill, Witting and Demetri (1963), Gyarmathy and Meyer (1965), Griffin and Sherman (1965), Duff and Hill (1966), Hill (1966), Stein (1967), Wegener and Parlange (1967), Deych and Filipov (1968), Dawson et al. (1969), Jaeger et al. (1969) Puzyrewski (1969), Wegener (1969), Roberts (1969), Chmielewski and Sherman (1970), Clumpner (1970), Barschdorff (1970, 1971), Wu (1972), Wegener, Clumpner and Wu (1972), Barschdorff et al. (1972), and Wu (1974).

with condensation associated with shock tube flows valid when the latent heat added to the gas stream is relatively small as used by Barschdorff (1975) and as seen in Section 6.

4 FLOW SYSTEMS FOR CONDENSATION RESEARCH.

a) Steady Nozzle Flow and Ludwieg Tube.

Nozzles provided the first data on steam condensation (e.g., Stodola 1927): they were used by Oswatitsch (1942) for his classical studies of nucleation, and have since been applied in many laboratories. Such Laval* nozzles are most useful in condensation research if the contour is designed for continuously expanding flow (e.g. Wegener 1964) rather than for a uniform Mach number distribution in the test section as found in supersonic wind tunnels. In the expansion, condensation causes a deviation of the pressure distribution from that observed in isentropic flow outside the boundary layers as determined from pressure surveys (see Section 2). Examples of such static pressure traces, $p(x)$, as obtained by a continuous pressure-distance

* The Swedish engineer de Laval introduced converging-diverging nozzles (Section 2b) in steam turbines in 1883.

survey in two different nozzles are shown in Fig. 4.1. The duration of the steady-state in such experiments is of lesser importance and continuous as well as intermittent wind tunnels are used. The choice of the mode of operation depends on the capacity of the vacuum equipment, high pressure supply, etc., and on the cost of the gas mixture to be expanded. In any case, the maximum expansion ratio of the nozzle, A/A^* , or the corresponding Mach number must be chosen to be beyond the initially estimated point of departure from the isentropic expansion as shown in Figs. 4.1 and 4.2. The nozzle is then designed with the aid of Eq. (2.31) and the corresponding values of the flow table in Appendix 1.

An advantageous application of a nozzle to condensation studies is provided by the so-called Ludwig tube (Ludwig 1955), a combination shock tube and nozzle facility. This device provides steady flows in the millisecond to second range (depending on the length of the supply tube) while operating without valves and other machinery. Here, non-equilibrium flows of poisonous or otherwise dangerous, or costly, gases can be produced since only a small amount of a carefully prepared mixture is required. The instrumentation for condensation studies (Wegener and Cagliostro 1973)

requires pulse techniques, however, it is in the range of common practice in experimental gasdynamics.

The application of the gasdynamic equations for diabatic flow (Section 3b) to experiments such as those of Fig. 4.1 leads to the results of Fig. 4.2. Ordinarily the assumption of dealing with a thermally and calorically perfect gas can be made and we obtain all local state parameters from a solution of the equations of motion in conjunction with known $A(x)$ and measured $p(x)$. In our example the heat addition due to condensation started at $x = 1.6$ cm and it is shown by the computed increase of the local total (stagnation) temperature above its value in the supply whose properties carry the subscript 01, to distinguish it from the computed local stagnation properties. Correspondingly, the irreversible character of the heat addition process is noted in a drop of stagnation pressure. It is important to recall that up to this point no assumptions on the condensation process were required and the thermodynamic state throughout the condensation zone could be computed from a simple experiment. Only after later applying Eq. (3.19) in Section 6 to data such as those of Fig. 4.2 shall we arrive at a determination of the condensate mass fraction.

Among the additional diagnostic methods, light scattering offers an attractive tool. In Fig. 4.3 from Stein (1969a) we see results for a cloud of water droplets obtained by laser light scattering beyond the nozzle exit of the equipment described in the reference and elsewhere (Stein 1969b). Similar data were obtained by Roberts (1969) and Clumpner (1971) who worked with ethanol. Since the wavelength of the laser $\lambda \gg r$, and multiple scattering is negligible, we are dealing with pure Rayleigh scattering, for which we have

$$\frac{I_{\theta}}{I_0} = \frac{h\ell^2}{R^2} \frac{16\pi^4}{\lambda^4} \cos^2\theta \left| \frac{m^2-1}{m^2+2} \right|^2 N \int_0^{\infty} r^6 f(r) dr, \quad (4.1)$$

where I_0 and I_{θ} are the intensities of the incident and scattered radiation respectively in units of energy/time. Furthermore, h and ℓ are the dimensions of the viewing window at angle θ at a distance R from the scattering volume. The index of refraction of the clusters is given by m , N is the total number of clusters per unit volume, and $f(r)$ is the normalized distribution function. Eq. (4.1), is valid for the case where the electric vector of the plane-polarized laser light is parallel to the plane of observation (E_{\parallel}), while for the case with the electric vector perpendicular (E_{\perp}), the $\cos^2\theta$ factor

would not appear. Fortunately, a second equation is at hand to link N and r as required to solve Eq. (4.1). Since we know (e.g. Wegener and Pouring 1964) that practically all the mass of the condensing vapor condenses in the condensation zone upon reaching the equilibrium state* at the observation station used in Fig. 4.3, we can write for the conservation of mass

$$\omega_{O} \rho_T = \frac{4}{3} \pi \rho_c N \int_0^{\infty} r^3 f(r) dr. \quad (4.2)$$

Different distribution functions for the radii can be matched to the light scattering signal in Eqs. (4.1) and (4.2). Figure 4.3, however, gives a simple evaluation assuming a delta function size distribution, i.e. a uniform radius for all clusters (see Section 6).

Finally, density distributions by interferometry, probing with pitot tubes, etc. have all been used in nozzles and we refer to such techniques in the list of papers in Appendix 2.

All these techniques enable us to determine the pressure and temperature on the isentrope at which the initial condensate appearance is noted.

* For proof see Section 6.

This "onset" of condensation yields the adiabatic supercooling, ΔT_{ad} , of Section 1, and Fig. 1.2, or with known $p_{\infty}(T)$, it permits us to compare the critical supersaturation $(p/p_{\infty})^*$ customarily employed in cloud chamber research. Figure 4.4 gives such "raw data" on water vapor condensation in steady nozzle flow for steam or in carrier gases. The sources of these data are listed in Table 4.1. The scatter of the points can be rationalized by remembering Eq. (1.1) and Fig. 1.4 since different cooling rates and different initial conditions are shown. However, a "Wilson line" shifted with respect to the equilibrium vapor pressure, $p_{\infty}(T)$, emerges.

b) Shock Tube.

There are several useful applications of the shock tube involving different regions of the flow (Fig. 2.2). Historically the first application of the shock tube to condensation studies (Wegener and Lundquist 1951) relates to the expansion fan between regions 4 and 3 in which the gas-vapor mixture undergoes an unsteady, isentropic expansion governed by the equations of Section 2c. There is some question on the quality of the flow set in motion by the fan. However,

experimental $p(t)$ histories agree perfectly with the prediction of the ideal theory provided an initial shift of the spatial coordinate has been made to account for inertial and other effects related to diaphragm rupture.* Flow fields were photographed by Glass and Patterson (1955) who show beautiful experimental $x-t$ diagrams with condensation fronts that are the unsteady analog to our steady nozzle flow photograph Fig. 1.1. Pressure-time histories without and with condensation, respectively, appear like the $p(x)$ graphs in Fig. 4.1 (Wegener 1975, Barschdorff 1975). At a given observation station, a pressure rise with respect to the ideal isentropic expansion and/or a light scattering signal reveal the onset of condensation and the history of the corresponding particle path (Fig. 2.2) can be computed as shown in Section 2. Usually the cooling rate is lower in such fans than in a nozzle. In fact, at a sufficient upstream distance from the diaphragm, the low cooling rates of cloud chambers may be duplicated. Finally, in order to avoid any effects of heat addition from condensation that may spread in both directions in the subsonic outflow of the

* This empirical correction can be avoided by simultaneous observations at two or more stations (Lee 1974).

driver section*, the onset of condensation may be arranged to coincide with the tail of the expansion fan as shown in Fig. 2.2 (Barschdorff 1975). Since it is normally impractical to shift the observation station, this condition can be achieved by a judicious choice of p_4/p_1 for Eq. (2.44). Onset data obtained in shock tubes may then be treated just like those for nozzles.

Other schemes are useful for condensation studies of materials such as metals that are vapors only at high temperatures. Placed in the driven section the substance of interest will first be heated and vaporized by the shock wave. Kung and Bauer (1971) have thus generated iron vapor at $T \sim 2,600$ K. Making use of earlier ideas on the so-called tailored interface technique (e.g. Wittliff et al. 1959), they produced controlled expansions in which to study the condensation by homogeneous nucleation of the previously

* Note that the tail of the expansion fan moves to the left in Fig. 2.2, i.e. $u_3 < a_3$.

vaporized iron vapor. However, these results as well as the use of the shock heated region 2 itself for the precipitation of e.g. lead held at constant temperature (Homer et al. 1971, Homer and Hurle 1972), have not yet led to satisfactory comparisons with nucleation theory.

c) Molecular Beam.

Becker and Henkes (1956) discovered that rapid expansions in high intensity molecular beams often lead to clustering of various species. Such beams are produced by expanding gases through hole-type nozzles into vacuum leading to very high Mach number flows in the free molecular regime ($Kn \gg 1$). The cooling rates in such expansions range up to 10^9 C/sec, and it has been shown that the steady-state assumption of classical nucleation theory is no longer valid under these circumstances (Andres and Boudart 1965). In spite of the fascinating cluster studies that this technique permits, we shall omit a discussion in this chapter. For one, our primary aim to compare well controlled gasdynamic continuum data with classical theory breaks down for the above reasons. Furthermore, Hagena (1974) has just published an excellent review

of the current status of condensation in molecular beams to which we shall defer.

5 EQUATIONS OF MOTION WITH HOMOGENEOUS NUCLEATION AND DROPLET GROWTH.

a) Gasdynamics.

In this section, we shall derive the governing equations for supersonic nozzle flow with condensation.* These equations will be derived under the assumptions laid out in Sections 2 and 3, and we shall focus on the special features of flows with condensation.

For the gaseous mixture (excluding the droplets of condensate), the equation of state, Eq. (2.5), for a perfect gas is assumed. Here, the unscripted symbols refer to the properties of the gaseous mixture, while the properties of the two-phase mixture are denoted by the subscript T. Since the condensate occupies a negligible volume compared with that of the gas phase, we may write

$$\rho_T = \rho + \rho'_C = \rho_i + \rho_v + \rho'_C . \quad (5.1)$$

We recall that ρ'_C is the condensate density referred to the volume of the gas phase, and ρ_T is the (apparent)

* Similar derivations, using slightly different notations, may be found in Wegener and Mack (1958), Stever (1958), Hill (1966), and Wegener (1969).

total density of the two-phase medium. This total density is, of course, meaningful only on length scales large compared with the average inter-droplet distance. With g , the mass fraction of condensate, we have:

$$\rho'_c = g\rho_T , \quad (5.2)$$

and

$$\rho_T = \rho/(1-g). \quad (5.3)$$

Instead of Eq. (2.8), the molecular weight of the gaseous mixture is to be computed from:

$$\frac{1}{\bar{\mu}} = \frac{1-\omega_0}{1-g} \frac{1}{\mu_i} + \frac{\omega_0-g}{1-g} \frac{1}{\mu_v} . \quad (5.4)$$

The continuity and momentum equations may readily be written in terms of ρ_T , or, using Eq. (5.3):

$$\rho u A / (1-g) = \text{constant} = \dot{Q} , \quad (5.5)$$

and

$$-dp = \frac{\rho}{1-g} u du , \quad (5.6)$$

respectively.

Equation (5.6) is equivalent to:

$$- A dp = \dot{Q} du . \quad (5.7)$$

The energy equation for unit volume of the gas-condensate mixture is:

$$d(\rho_T u^2/2 + \hat{h}_T) = 0 . \quad (5.8)$$

Here, \hat{h}_T is the enthalpy per unit volume of the two-phase medium. It may be written as:

$$\hat{h}_T = \rho_i h_i + \rho_v h_v + \rho'_c h_c , \quad (5.9)$$

where h_i , h_v , and h_c are the enthalpy per unit mass of the inert gas, vapor and condensate respectively. The enthalpies of the vapor and condensate, are related by their temperature difference and the latent heat of condensation.* Thus:

$$h_v - h_c = L + c_c (T - T_c) , \quad (5.10)$$

where c_c and T_c are the specific heat and temperature, respectively, of the condensate. In most cases, we may safely ignore the temperature difference between the gas phase and the condensate without introducing a significant error in the energy equation. Under this assumption, we have

$$h_v - h_c = L , \quad (5.11)$$

* Here we shall again set $L=L_\infty$; note Eq. (3.19).

and the energy equation becomes

$$d[\rho_T u^2/2 + \rho_i h_i + \rho_v h_v + \rho_c'(h_v - L)] = 0 \quad (5.12)$$

With the definition of ω_o , the mass fraction of vapor in the supply which is assumed to be free of condensate, we get

$$d[u^2/2 + (1-\omega_o)h_i + \omega_o h_v - gL] = 0 \quad (5.13)$$

Defining c_{po} as the constant-pressure specific heat of the vapor-carrier gas mixture in the supply, we arrive at the energy equation for flows with condensation:

$$d[u^2/2 + c_{po} T - gL] = 0 \quad (5.14)$$

Had we not assumed equal temperature for the gas phase and condensate, we would have arrived at a similar equation with L replaced by \tilde{L} where

$$\tilde{L} = L + c_c(T - T_c) \quad (5.15)$$

For a conservative estimate, we figure* the error in the quantity in the square brackets in Eq. (5.14) due to the replacement of \tilde{L} by L to be about 0.1%, which is negligible. Hence, we conclude that in the energy equation for gas flow, we may ignore the temperature difference

* For typical conditions prevailing in steam nozzles, $T = 300$ K, $T_c = 320$ K, $g = 10^{-2}$, $u = 500$ m/sec.

between the droplets and the gas. The question of droplet temperature arises again in the calculation of growth rates where it will be necessary to evaluate the droplet temperature.

The presence of the term gL in the energy equation, Eq. (5.14) in contrast to Eq. (2.19) suggests that vapor condensation is equivalent to the addition of heat $q = gL$ to unit mass of the flow. The equation of state, Eq. (2.6), the continuity equation, Eq. (5.5), the momentum equation, Eq. (5.6) or (5.7), and the energy equation, Eq. (5.14) now complete the gasdynamic description of the flow with condensation. These equations reduce to those for perfect gases derived in Section 2 when g is identically zero. Here, g is left unspecified, and we must turn to the kinetics of the condensation process to determine its value.

b) Condensation Kinetics.

The mass fraction of condensate $g(x)$ may be computed from

$$g(x) = \frac{4\pi}{3} \frac{\rho_c}{Q} \int_{-\infty}^x J(\zeta) A(\zeta) r^3(\zeta, x) d\zeta . \quad (5.16)$$

Here, J and A are the nucleation rate and the (effective) nozzle cross-sectional area, respectively, with both as functions of the position along the nozzle. The quantity $r(\zeta, x)$ is the final radius at x of a droplet nucleated at ζ , and it is given formally by:

$$r(\zeta, x) = r(\zeta, \chi) \Big|_{\chi=\zeta} + \int_{\zeta}^x \frac{\partial r(\zeta, \chi)}{\partial \chi} d\chi . \quad (5.17)$$

The differential $\partial r / \partial x$ is related to the droplet growth rate by:

$$dr/dt = u(\partial r / \partial x) , \quad (5.18)$$

for steady flow. The first term on the right hand side of Eq. (5.17) may be identified as the initial radius of the droplet at its formation, i.e.:

$$r(\zeta, \chi) \Big|_{\chi=\zeta} \equiv r_0(\zeta) . \quad (5.19)$$

The integrations in Eqs. (5.16) and (5.17) are to be performed along the particle path which in our case is equivalent to the nozzle axis. The physical foundation of Eqs. (5.16) and (5.17) have been explained before.

Nucleation Rate Equations:

Despite the current controversy over the physical

model of homogeneous nucleation theory, the so-called "classical theory", developed by Becker and Döring (1935), Volmer (1939), Frenkel (1946), et al., is found to give remarkable qualitative agreement with many experiments as will be seen in Section 6. For this reason we chose the classical theory as the basis for incorporation in calculations performed with Eq. (5.16). A convenient form for this steady state nucleation rate is given by:

$$J_{cl} = \sqrt{\frac{2}{\pi}} \frac{N_A^{2/3}}{R^2} \left(\frac{p_v}{T}\right)^2 \sqrt{\frac{\sigma_\infty \mu_v}{\rho_c}} \exp \left\{ -\frac{n^* \ln(p_v/p_\infty)}{2} \right\}, \quad (5.20)$$

where

$$n^* = (4\pi/3)\rho_c (N_A/\mu_v)(r^*)^3, \quad (5.22)$$

$$\text{and } r^* = (2\sigma_\infty \mu_v) / [RT\rho_c \ln(p_v/p_\infty)]. \quad (5.23)$$

In these equations, the quantities with an asterisk pertain to clusters of the critical size given by Eq. (5.23), the well-known Gibbs-Thomson equation.[†] It can be shown that clusters of this critical size are in unstable equilibrium with the vapor and this size must be achieved to ensure the probability of further unlimited growth of a cluster. In cgs units Eq. (5.20) reduces to

[†]Confusion with respect to the asterisk assigned to states at the nozzle throat, etc. must be avoided.

$$J_{cl} = 5.4 \times 10^{19} \left(\frac{p_v}{T} \right)^2 \frac{(\sigma_\infty \mu_v)^{1/2}}{\rho_c} \exp \left\{ - \frac{n^* \ln(p_v/p_\infty)}{2} \right\}. \quad (5.24)$$

The liquid drop model of the classical homogeneous nucleation theory, i.e. the so-called capillarity assumption, has been under question for some time. The work of Kuhrt (1952a, 1952b), Lothe and Pound (1962), Dunning (1965), and Reiss (1970), represents various models to incorporate the contributions from statistical mechanics considerations to the energy of formation of the cluster and, hence, to the rate of homogeneous nucleation. The different ideas have resulted in rates which may vary by large factors. We shall not discuss the relative merits of the competing theories. Rather, interested readers are referred to the various viewpoints in the readily available review articles of Dunning (1969) and Lothe and Pound (1969) in the first volume of this series of monographs, and those by Wegener and Parlange (1970), and Reiss (1970). Here, we shall simply write down the final results of the formalism in a convenient general form which may be used to compute the nucleation rate according to any of the models presented. Assuming that partition functions for translation and rotation of the clusters can be computed in the standard manner, we write:

$$J = \Gamma J_{cl} \quad (5.25)$$

where
$$\Gamma = \left[\left(\frac{2\pi n_c^* m_c kT}{h^2} \right)^{3/2} \frac{kT}{P_v} \right] \left[\left(\frac{8\pi^2 I^* kT}{h^2} \right)^{3/2} \sqrt{\pi} \right] / q_{rep}^* ,$$
 (5.26)

and
$$I^* = \frac{2}{5} n_c^{*5/3} m_c \left(\frac{3v_c}{4\pi} \right)^{2/3}$$
 (5.27)

is the moment of inertia of a spherical critical cluster. The "replacement factor", q_{rep}^* , is introduced in the above equation (Lothe and Pound 1966) to account properly for the changes in energy in the internal degrees of freedom of the condensate when a cluster is formed from the bulk.[†] Primarily solutions for the models for q_{rep}^* are the subject of the current debate and this factor is thus left open in our method of calculation.

On the other hand, the validity of the concept of a macroscopic surface tension for the small clusters has been questioned. Since the cube of the surface tension of the cluster enters the exponent of Eq. (5.20) via Eqs. (5.22) and (5.23), its importance is self-evident. Theoretical treatments of surface tension of small clusters (Tolman 1949, Kirkwood and Buff 1949, and Oriani and Sundquist 1963, Benson and Shuttleworth 1951) lead to

[†] The coefficient Γ in Eq. (5.25) will later appear again in Eq. (6.1) as an empirical factor to match experiment and theory.

sharply contrasting results. However, we consider it to be consistent with the definition of q_{rep} to include in q_{rep} the possible effects of variation of surface tension with size. Thus we set $\sigma \equiv \sigma_{\infty}$, and apply the bulk value of the surface tension in the rate equations relegating all uncertainties to the coefficient Γ .

Thus we consider Γ as the theoretical correction factor for the classical homogeneous nucleation rate to account for the contribution to the energy of formation of a cluster from statistical mechanical as well as thermodynamic sources. Volmer's work, etc., implies, of course, $\Gamma = 1$.

In addition to the steady state assumption Eqs. (5.20) and (5.25) are both based on the assumption that the sub-critical clusters are in thermal equilibrium with the ambient gas during their growth towards the critical size. We recall that this assumption is valid only in the case when a large quantity of inert carrier gas is present to facilitate the dissipation of latent heat of condensation from the cluster. In reality, however, the finite heat transfer rate ought to be taken into consideration in nucleation kinetics calculations to obtain a nonisothermal nucleation rate, J_{noniso} . This effect was first noted by Kantrowitz (1951), and a more detailed treatment was given by Feder et al. (1966)

who modified the classical kinetic treatment of homogeneous nucleation to account for the temperature differences between the cluster and ambient gas due to finite heat transfer rates. Their result may be summarized as:

$$J_{\text{noniso}} = [b^2 / (b^2 + d^2)] J_{\text{iso}}, \quad (5.28)$$

where

$$b^2 = \frac{\gamma_v + 1}{2(\gamma_v - 1)} + \frac{(1 - y_v)}{y_v} \sqrt{\frac{\mu_v}{\mu_i} \frac{\gamma_i + 1}{2(\gamma_i - 1)}}, \quad (5.29)$$

and

$$d^2 = \left[\frac{L\mu_v}{RT} - \frac{1}{2} - \left(1 - \frac{T}{\sigma} \frac{\partial \sigma}{\partial T}\right) \ln \left(\frac{P_v}{P_\infty} \right) \right]^2. \quad (5.30)$$

and J_{iso} is the "isothermal" nucleation rate. For J_{iso} we may choose the classical rate, Eq. (5.20) or the rate derived from the statistical mechanics treatment, Eq. (5.25).

Droplet Growth Equations:

After a cluster of the critical size given by Eq. (5.23) has been formed by nucleation, its further growth by vapor condensation on its surface is possible until thermodynamic equilibrium is attained. We have mentioned that the early stage of droplet growth, which is crucial in the determination of the onset of condensation, takes place

under free molecule flow conditions. Resistance to droplet growth in FMF arises solely at the gas-droplet interface and the transfer processes across this interface are characterized by the mass, momentum and thermal accommodation coefficients. This situation contrasts with droplet growth under continuum flow conditions ($Kn \ll 1$), where the primary barrier to growth is given by vapor diffusion and heat conduction.*

The saturation vapor pressure, p_r , of a droplet of a pure liquid with radius r is given by solving the Gibbs-Thomson equation Eq. (5.23) for the vapor pressure:

$$p_r(T) = p_\infty(T) \exp \left\{ \frac{2\sigma\mu_v}{RT\rho_c r} \right\}. \quad (5.31)$$

This and the other characteristic properties of droplet growth are indicated schematically in Fig. 5.1. Thus, a droplet of size r is in equilibrium with the surrounding vapor if the temperature of the droplet and vapor are equal and if the partial pressure of the vapor p_v is equal to p_r . However, this equilibrium is unstable. A larger droplet will tend to grow whereas a smaller one

* In accordance with the assumption of no slip between the droplets and the gas stream, we need to consider only droplet growth in a quiescent medium, i.e., bulk convective motion of the surrounding gas is absent.

will evaporate in the same surroundings.

The condensation of vapor molecules on the surface of a droplet results in the release of latent heat of condensation which is then dissipated from the droplet.* Therefore, a droplet growing in a supersaturated environment will generally have a surface temperature higher than that of the surrounding medium, but lower than the saturation temperature of the droplet corresponding to the ambient vapor pressure. The vapor pressure exerted by the droplet will then lie between the free stream vapor pressure p_v , and the saturation vapor pressure, $p_r(T)$, at temperature T over a spherical surface of radius r , as given by Eq. (5.31). These limits are also depicted in Fig. 5.1. The overall mass exchange rate on a droplet arises from the difference between the rates at which vapor molecules arrive (condensation) and leave (evaporation) the surface.

Droplet growth behavior under continuum flow conditions has been studied by many investigators, and it has been reviewed by Hidy and Brock (1970). Of these results, a convenient formula for droplet growth

* We recall that, for many liquids at their normal boiling points, the latent heat of condensation per molecule is about $12 kT$ (Trouton's rule).

rate in a quiescent, continuous medium obtained by Gyarmathy (1963) is attractive in our situation. He solved simultaneously the equations of vapor diffusion and heat conduction between the droplet and the surrounding medium and expressed the droplet growth rate as a function of the droplet radius, the temperature, pressure and the composition of the surrounding gas. The fact that the surface temperature of the droplet does not appear explicitly in Gyarmathy's formula for droplet growth in a continuum makes his results more useful than other results, since the surface temperature is unknown a priori.

The droplet growth rate in FMF may be expressed as

$$\frac{dr}{dt} = \alpha \frac{m_c}{\rho_c} \left[D(p_v, T) - De(T_d, r) \right], \quad (5.32)$$

where

$$D(p_v, T) = p_v (2\pi m_c kT)^{-\frac{1}{2}}, \quad (5.33)$$

is the impingement rate of vapor molecules from kinetic theory, $De(T_d, r)$ is the evaporation rate of a droplet at temperature T_d and radius r , and α is the mass accommodation coefficient. Under the assumptions underlying the principle of detailed balancing, this evaporation

rate may be taken (Knudsen 1915, Paul 1962) to be equal to the impingement rate on the droplet by its saturated vapor at the same temperature.

Thus:

$$De(T_d, r) = D \left[p_r(T_d), T_d \right] = \frac{p_r(T_d)}{\sqrt{2\pi m_c k T_d}}, \quad (5.34)$$

where $p_r(T_d)$ is again given by Eq. (5.31). Alternatively, we may define an effective condensation coefficient that formally accounts for evaporation by

$$\alpha' = \alpha \left[1 - De(T_d, r) / D(p_v, T) \right], \quad (5.35)$$

and rewrite Eq. (5.32) as:

$$dr/dt = \alpha' (m_c / \rho_c) D(p_v, T) . \quad (5.36)$$

Since the temperature of the drop* is unknown, it must be determined by energy considerations. Hill (1966) derived the following equation for the energy balance of this droplet:

$$\begin{aligned} \alpha K_v k (DT - De T_d) / m_c + (1 - \alpha) K_v k D E_v (T - T_d) / m_c + D_i K_i k \xi_i (T - T_d) / m_i \\ \approx h_c(T_d) \alpha D (1 - De/D) , \end{aligned} \quad (5.37)$$

* We assume the temperature inside these droplets to be uniform. It can be shown that the temperature equalization time inside the small droplets under consideration ($r < 1000 \text{ \AA}$) is extremely short, of the order of 0.1 μsec or shorter.

where $K = (\gamma+1)/[2(\gamma-1)]$ so that the product KkT denotes the average energy of impinging molecules. The term $h_c(T_d) = [\gamma_v/(\gamma_v-1)]kT_d/m_c - L(T_d)$ is the enthalpy of the condensate at temperature T_d . The first term on the left hand side accounts for the difference in energy carried by the condensing and evaporating molecules. By definition of the thermal accommodation coefficient ξ , the second and third terms denote the energy transferred by the reflection of vapor and inert carrier gas molecules, respectively, at the droplet surface. The term on the right hand side is the rate of energy accumulation of the drop neglecting the relatively small contributions from temperature change and surface energy of the drop (Hill 1966).

Together with Eq. (5.31) for the equilibrium vapor pressure over a curved surface, Eqs. (5.35), (5.36) and (5.37) may be solved simultaneously for the three unknowns dr/dT , T_d , and $p_r(T_d)$. Owing to the complexity of these equations, an iteration procedure is necessary to obtain the growth rate dr/dt , (e.g., Hill 1966, Jaeger et al. 1969, Dawson et al. 1969).

Fortunately, for most cases of practical interest, such an exact solution is not necessary and useful approximate solutions have been obtained by Wu (1972). For

example, when a large quantity of inert carrier gas is present, the droplet remains practically in thermal equilibrium. Typically in moist air, a water molecule undergoes roughly a thousand collisions with inert gas molecules for each encounter with another water molecule which may lead to condensation. Hence, $T_d = T$, the condition of the droplet is represented by point 2 in Fig. 5.1, and we have:

$$\alpha' = \alpha \left[\frac{1 - p_r(T)}{p_v} \right]. \quad (5.38)$$

Next, when the droplet and the ambient gas are nearly in thermal equilibrium i.e. its state is near point 2 in Fig. 5.1, an approximate expression for α' has been obtained:

$$\alpha' = \frac{\alpha [1 - p_r(T)/p_v]}{1 + \frac{\alpha}{K_v} \frac{p_r(T)}{p_v} \frac{Lm_c}{kT} \frac{Lm_c/kT - 1/2}{[1 - (1-\alpha)(1-\xi_v)] + \xi_i \frac{K_i}{K_v} \frac{p_i}{p_v} \left(\frac{m_c}{m_i}\right)^{3/2}}} \quad (5.39)$$

Equation (5.39) is valid only when $|T_d - T|/T \ll 1$, however, under practical conditions this requirement is satisfied when

$$\left| \frac{kT_p}{p_v m_c L} + \frac{m_c L}{kT} \right| \gg 1. \quad (5.40)$$

which is normally the case.

On the other hand, for a high latent heat of condensation of the vapor, or a low concentration of inert carrier gas, the droplet temperature approaches the saturation temperature for the droplet, indicated by point 3 in Fig. 5.1. In the limit when $T_d = T_s(r, p_v)$, the saturation temperature at p_v over a droplet of radius r , we have,:

$$\alpha' = \alpha(1 - \sqrt{T/T_s}) \quad (5.41)$$

For droplet temperatures close to the saturation temperature, $|T_d - T_s| \ll T_s$, we have:

$$\alpha' = \frac{\alpha \left\{ 1 - \sqrt{\frac{T}{T_s}} \left[1 - \frac{L(T_s)m_c}{kT_s} \left(1 - \frac{T}{T_s} \right) \right] \right\}}{1 + \frac{\alpha}{K_v} \sqrt{\frac{T}{T_s}} \frac{L(T_s)m_c}{kT_s} \frac{L(T_s)m_c/kT - 1/2}{[1 - (1-\alpha)(1-\xi_v)] + \xi_i \frac{K_i p_i}{K_v p_v} \left(\frac{m_c}{m_i} \right)^{3/2}}}} \quad (5.42)$$

Equations (5.38), (5.39), (5.41) and (5.42) cover a substantial part of the entire temperature range of a growing droplet. In addition, the "near equilibrium" and "near saturation" approximations, Eqs. (5.39) and (5.42) may also be used to compute the evaporation rate of a droplet in an unsaturated atmosphere, resulting in a negative α' . These equations are explicit expressions for α' in terms of measurable ambient

conditions only, therefore they offer an attractive alternative to solving the mass and heat transfer equations simultaneously.

Notice that the terms entering Eq. (5.16) and the nucleation and droplet growth rate equations are generally functions of the thermodynamic state of the two-phase system under consideration. The state of the system is determined by the gasdynamics of the flow, which, in turn, is influenced by the condensation process. It is clear that the kinetics of phase change is coupled with the gasdynamics of the flow process. Equations (5.16) and (5.17) must therefore be integrated simultaneously with the proper gasdynamic equations of motion and the mass fraction of the condensate will then emerge as part of the complete solution.*

6 EXPERIMENT AND THEORY

We can now discuss typical results on homogeneous nucleation as obtained by gasdynamic methods. At first, general examples will

* Computer programs have been written at our laboratory (Wu 1974) for this problem and several variants. They are available upon request.

be given on the functional relationships between experiment and theory. Next, a data collection will be provided with many results newly evaluated by identical methods of data reduction. While we rely largely on information from our laboratory in the first part, the tabular results on several substances which have not been published previously will include experiments from other sources provided that the "raw data" could be retrieved from the publications. It is believed to be imperative to treat experimental findings uniformly because of the great sensitivity of various parameters in nucleation theory to the choice of various properties. Finally, all comparisons have been screened to comply with the assumptions implicit in the previous sections including the following criteria.

One-dimensional steady or unsteady flow prevails.
Viscous effects and turbulence in the free stream are unimportant.

The flow parameters are known throughout the condensation region (or at least at the onset of condensation).

The heat addition by condensation does not lead to thermal choking, i.e. no shock waves appear.

Continuum flow prevails.*

Cooling rate and time scales are sufficiently moderate for the steady-state assumption of the classical nucleation theory to apply.*

The presence of aerosols is unimportant.

Vapor impurities are of sufficiently low level that binary nucleation is unimportant.

a) General Results.

Properties at the onset of condensation. Flow experiments provide raw data such as those of Fig. 4.1 directly yielding the onset conditions as shown in Fig. 4.4. An understanding of the state parameters through the condensation zone (Fig. 4.2) can moreover be derived by solving the diabatic flow equations with heat addition as described in Section 3b.** Since the heat addition is due to condensation, Eq. (3.19) can be applied to the data of Fig. 4.2. Thus, the condensate mass fraction as a function of distance, (or time, (see Eq. (2.32)), can be determined directly as shown in Fig. 6.1. The shaded area describes the uncertainty of $g(x)$ resulting from experimental uncertainties. It is this remarkable resolution of the rate of condensation beyond the critical supersaturation that sets the nozzle method apart from the cloud chamber. However, $g(x)$ cannot yet be

* This assumption again rules out the inclusion of clustering in high intensity molecular nozzle beams e.g. Hagena (1974).

** The variations in molecular weight, etc. of the mixture as a result of change in mixture composition may be incorporated in the equation without difficulty.

computed independently based on first principles by the inclusion of nucleation and growth equations. To apply the equations developed in Section 5 for comparison it is therefore useful to introduce an empirical adjustment factor, Γ , such that

$$\Gamma = J_{\text{exp}}/J_{\text{th}} , \quad (6.1)$$

where, J_{th} symbolizes a theoretical expression for the nucleation rate such as Volmer's Eq. (5.24) or some other expression for the nucleation rate such as Eq.(5.28). For a **given** experimental environment and **nozzle** geometry, a complete solution of the equations can be repeated for an estimated range of values of Γ in Eq. (6.1). That value of Γ can then be chosen for which the strong increase in computed nucleation rate coincides with the observed onset of condensation. This location in space (nozzle) or time (shock tube), can be more clearly defined moreover as a match of the observed and the computed condensate mass fraction e.g. at the location of the departure of the pressure from the isentrope in Fig. 4.1.

We recall that the symbol, Γ , was previously introduced in Eqs. (5.25) and (5.26) as a ratio of partition functions. The empirically determined factor, Γ , of Eq. (6.1) as obtained from a complete

solution of nucleation and growth equations in comparison with experiment can now be interpreted as an experimental solution for Eq. (5.26). This proposal will be elucidated in the following Section 6b. At the onset of condensation here defined as the location in Fig. 6.1 where $g = 0.7 \times 10^{-3}$ *, we note $\Gamma = 10^5$ for $\sigma = \sigma_\infty$ in Eqs. (5.20) and (5.25). For ethanol, the temperature at the onset of condensation lies above the triple point permitting the use of tabulated surface tension values for the bulk liquid. In this fashion different versions of the theory of nucleation may readily be compared with experiment. The well-known "go" versus "no go" feature of nucleation is again demonstrated in Fig. 6.1 since the nucleation rate plotted quickly attains a maximum of about $J \sim 10^{19} \text{ cm}^{-3} \text{ sec}^{-1}$ at the measured onset of condensation. About 40 μsec before the vapor sample reaches this location, the rate of nucleation was as low as $J = 1$ per earth volume per age of the earth! While the cloud chamber experiment may at best establish the critical supersaturation of the onset in an undisturbed small central volume

* This relatively higher value of the condensate mass fraction than those used later for water vapor is required since the latent heat of ethanol is lower and consequently more condensate is needed to measurably disturb the isentropic flow by heat addition. In fact, if a diagnostic method such as light scattering permits the location of the onset of condensation experiments for vanishing heat addition can be performed permitting the application of the isentropic properties.

in the chamber, the "sensitive volume" (Kassner and Schmitt 1966), the gasdynamic evaluation permits a detailed resolution of this rapid process.

Properties of the condensation zone. Once the measured onset conditions have been matched by theory, a further complete calculation of nucleation and growth yielding the accretion of the condensate mass fraction beyond the onset location can be computed from data such as those of Fig. 4.2. These results for $g(x)$ agree well with the measurement as shown in Fig. 6.1. The calculation of droplet growth with $\alpha = 0.7$ in Eqs. (5.36) and (5.39) gives excellent results.* In this instance nucleation and growth follow each other, each taking about 20 μsec . We note the fast build-up of the number of particles and the rapid drop of the nucleation rate resulting from the decline in saturation ratio in the condensation zone caused by vapor depletion. The number density of the particles again drops slightly due to the ensuing expansion while coagulation can be shown to be negligible in the condensation zone (Wegener and Stein 1969). Finally, at the end of the condensation zone, thermodynamic equilibrium

* The choice of $\alpha = 0.7$ is reasonable in the light of recent work on this coefficient (Mills and Seban 1967, Lednovich 1974).

is again established when nearly all the ethanol has condensed, i.e., $\omega_0 \approx g$. In fact the partial pressure of ethanol vapor required to maintain $p_v/p_\infty = 1$ is negligible at these low temperatures.

With the same methods, we can now interpret light scattering results in greater depth than shown in Fig. 4.3. Computed distribution functions for cluster populations emerge as by-products of these calculations as plotted in Fig. 6.2. Most of the droplets are roughly of the same size reflecting the fact that most of them originated on nuclei of critical size formed at the location of the peak value of the nucleation rate slightly beyond the onset location. Similar results are available for H₂O in air (Wegener and Stein 1969), and pure steam (Barschdorff et al. 1974). In all situations the computed and measured drop sizes agree well.

Cooling rate. At the high cooling rates in rapid expansions the question arises if the steady-state nucleation rate can be established in the short time available. These induction times have been variously estimated as reviewed e.g. by Courtney (1962), and Andres and Boudart (1963). Ordinarily, such time scales are estimated to be of the order of a few microseconds, however, Courtney (1962) suggests larger values at the low temperatures in

question. At any rate with gasdynamic techniques, again with the striking exception of the high intensity molecular beams, the time of persistence of the supersaturated state and the time elapsing in the actual condensation zone, e.g. Fig. 6.1, appear to be significantly above the induction time.* We can demonstrate this fact without resort to basic theory by calculations on the effect of cooling rate for condensation in two nozzles of different cooling rates. Figure 4.1a shows an experiment in a nozzle with a cooling rate computed from Eq. (2.34) of $dT/dt = - 0.7 \text{ C}/\mu\text{sec}$. With an empirical value of $\log_{10} \Gamma = 4.7$ and $\alpha = 0.6$ in Eqs. (5.25), (5.36), and (5.39) respectively, together with the equations of motion with heat addition we obtain the calculated results for pressure, also shown in Fig. 4.1a. This calculation again gives excellent agreement between experiment and theory. Next we apply the same values of Γ and α without any further adjustment to a second complete calculation for the conditions of the experiment shown in Fig. 4.1b. Here we deal with a nozzle with a cooling rate of $dT/dt = - 2.8 \text{ C}/\mu\text{sec}$,

* A Damköhler parameter giving the ratio of a characteristic flow time to the induction time or the time elapsed in the condensation zone offers itself. Such a discussion is of particular interest in the nozzle flow treated as a nonequilibrium flow with a single relaxing mode without regard to the physical mechanism of condensation (Wegener 1975).

and again excellent agreement with the experimental result is achieved. Although the cooling rates differ only by a factor of four between the two nozzles, it appears that the theory yields satisfactory results in this range of expansion rates. If the steady-state assumption were not valid in these rapid expansions, such agreement would be quite unlikely.

Approach to the critical point. Nucleation theory implies (Volmer 1939) that an initial step towards the build-up of critical nuclei involves the formation of a dimer by



where M represents a third body. The start of nucleation is therefore tied to tertiary collisions. It is interesting to note that in fact in the onset region of typical nozzle experiments such as shown in Figs. 4.1 or 6.1, triple collisions are about one order of magnitude more frequent than the nucleation rate in this range. With the collision frequency depending strongly on pressure, it is expected that the supersaturation decreases at increased pressure, in particular if the critical point is approached. Moreover, the surface tension decreases to vanish at the critical temperature. This feature of the theory is indeed borne out by nozzle and

shock tube experiments with steam as seen in Fig. 6.3. The results of Gyarmathy (1973) at temperatures approaching the critical point are particularly remarkable since they were obtained in situ in a steam turbine operating in a modern power plant (Karlsruhe, Germany) with pressures at the condensation onset of up to 75 atmospheres. Additional evaluation of these high pressure data is difficult since the ideal gas law assumptions are inapplicable for steam once the pressures in the flow exceed about one atmosphere.

Carrier gas effects.

The isothermal assumption implicit in the derivation of Eq. (5.20) is physically well realized by mixing the vapor with an excess of a non-condensing carrier gas as found e.g., in the moist air in a cloud chamber. In recent shock tube experiments on H₂O condensation mixed in He, A, and air, shown in Fig. 6.4, Barschdorff (1975) verified the absence of carrier gas effects. The slight differences

noted can be rationalized in view of the different values of the ratio of the specific heats, γ , of the gas-vapor mixtures leading to slightly different cooling rates in the centered expansion in the shock tube driver chamber (see Section 2c). Recalling our discussion on droplet growth we note that the number of collisions available exceeds the number required to insure thermal equalization of cluster and surrounding gas mixture demonstrating that the properties of the carrier become unimportant.

Non-isothermal condensation. The simplifying condition of equal temperature of drops and vapor ceases to be valid in pure vapor condensation. Here, the application of the classical, isothermal theory, e.g. Eq. (5.20) with $\sigma = \sigma_\infty$ and $\alpha = 1$ to a complete solution of the equations for typical steam nozzle flow in nozzles yields $\Gamma \approx 10^{-5}$, i.e. the experimental rate of condensation appears to be appreciably slower than that predicted by Volmer's equation. Experiments of many steam investigators compared with theory as listed by Barschdorff et al. (1972) prove this point and new calculations are given in Table 6.2. On an identical basis, the comparison of theory and experiment

(Arthur 1952) for pure nitrogen yields $\Gamma \sim 10^{-6}$ also seen in Table 6.2. Oddly enough until recently (Barschdorff et al. 1972), this fact appears to have been overlooked excepting a general remark in the work of Deych et al. (1969a) who pointed out that the theory yields condensation rates for steam "which are too high by several orders of magnitude" in comparison with experiments. Usually this discrepancy between the theory and the experiment was masked by artificially "slowing down" the condensation rate in the theory by applying low values of the condensation coefficient to the growth law (Hill 1966), or resorting to the unjustified introduction of a "friction factor" in the momentum equation (Campbell and Bakhtar 1973). We should in fact expect values $0.1 < \alpha < 1$ (Mills and Seban 1967) for the mass accommodation coefficient and boundary layer effects can be assumed to be negligible or calibrated via the effective area concept (Section 2). The apparent low values of Γ must therefore be accounted for otherwise.

Feder et al. (1966) based on prior work (Kantrowitz 1951) treated the non-isothermal build-up of clusters in pure vapors by deriving a new preexponential factor for the nucleation rate as shown in Eq. (5.28). This non-isothermal factor yields a lower nucleation rate since some of the vapor molecules that collide

with the droplets do not condense and they now carry off the thermal energy arising from the latent heat.* An application of this result to steam condensation is demonstrated in Fig. 6.5. At large values of the condensation coefficient, for the growth rate of water droplets beyond their critical size, the rate of nucleation is slowed with respect to the isothermal equation by non-isothermal effects by about three orders of magnitude. A proper combination of the non-isothermal theory and a reasonable value of α provide good estimates for technological purposes of the onset of condensation in steam nozzles.

Finally, additional features of the experiments with varying vapor mass fractions (Barschdorff 1975) compared with the non-isothermal, classical nucleation theory (with $\sigma = \sigma_{\infty}$ and $\alpha = 1$ in the growth law) are seen in Fig. 6.4. Values for Eq. (6.1) with the non-isothermal theory are plotted as a function of the initial specific humidity in the range of $0.004 < \omega_0 < 1$, with the previously discussed results from different carrier gases. In the shock tube experiments, the cooling rate

* This effect is, of course, equivalent to the use of a low "sticking coefficient", however, the physical process is of a different origin, see Section 5.

is lower by about one order of magnitude (10^5 vs. 10^6 C/s) than in the nozzle experiments of Fig. 6.1. The puzzling result of Fig. 6.4 is the fact of a variation of $10^6 < \Gamma < 1$ between the limits of low vapor concentration to pure steam. In light of our previous thoughts, one might expect $\Gamma = \text{constant}$ (although possibly $\Gamma \neq 1$) irrespective of the initial humidity since critical drop sizes, expansion rates, initial conditions, etc. are roughly equal. Although the non-isothermal theory of nucleation predicts the proper general trend as seen in Fig. 6.5, the dominant exponential term in the rate equation is, however, unaltered in this work. Here the surface tension enters in the third power (Parlange 1970). The calculations in Fig. 6.4 were performed for a $\sigma_\infty(T)$ function obtained from tables for the temperature of the gas flow as obtained for the isentropic expansion. However, the droplet is warmer than its surroundings affecting its surface free energy. Since the droplet temperatures have not been calculated, the trend noted in Fig. 6.4 remains quantitatively unexplained.

Small cluster properties. Finally, some qualitative hints can be provided on the properties of small clusters by making use of the phenomenological accuracy of the classical theory of nucleation. By "small" we consider here the typical critical H₂O drops or clusters whose critical radii as computed with Eq. (5.23) of $4 < r^* < 12 \text{ \AA}$ for typical onset data contain about $9 < n^* < 250$ molecules (see Table 6.1) as obtained from Eqs. (5.23) and (5.22). Trends of experimental data can be deduced by assuming that the pre-exponential in Eq. (5.20) is constant for a given expansion to get:

$$J = \text{const.} \exp \left[- \text{const.} (\sigma_{\infty}/T)^3 \ln^{-2}(p/p_{\infty}) \right]. \quad (6.3)$$

If we further set $\sigma_{\infty} = \text{const.}$ and $J = \text{const.}$ at the onset of nucleation, we expect the function:

$$\log(p/p_{\infty}) = f \left(T^{-2/3} \right), \quad (6.4)$$

to be a straight line. In fact cloud chamber results as reproduced in Fig. 6.6 verify this trend. We find moreover $\log(p/p_{\infty}) = 0$ for $T = \infty$ as expected formally. In the same figure, we show experimental data on water vapor condensation in nozzles and shock tubes from a variety of sources. For simplicity, the vapor pressure was taken to be that over ice if $T < 273 \text{ K}$ in

order to have a uniform basis for evaluation of the critical supersaturation. Many other results were studied for H₂O and other vapors in the same manner and in general the trends are similar to those of

Fig. 6.6. In line with the empirical function of Eq. (1.1) and Figs. 1.3 and 1.4, lower humidities and/or higher cooling rates respectively lead to a larger critical supersaturation. Conversely, the two effects may counteract each other. In general, it is found that given sets of experiments lie on straight lines, however, the lines do not point to the origin of the coordinate system, as formally required by Eq. (6.3). Similar results are noted for steam as seen in Fig. 6.7.

A straight line is noted even when the vapor behavior departs drastically from the perfect gas behavior as seen for the high pressure data of Gyarmathy et al. (1973). His results point to the critical point where we expect $\log(p/p_{\infty}) = 0$ at $T_{\text{crit}} = 374$ C. It is inviting to relate the slopes of these lines, their intercepts, etc. to additional features of the theory. The results of Figs. 6.6 and 6.7 show that the "constant" preceding the exponential on the right hand side of Eq. (6.3) is itself

a function of the temperature for the correlation given. Direct use of Eq. (6.3) including a variable bulk surface tension does not, however, materially alter the trend of the curves shown. It therefore appears that the surface tension of the clusters is not an important variable in this range pointing to a structure whose properties depend little on temperature.*

Binary Nucleation.

Finally, gasdynamic methods have been applied just like the cloud chamber to a study of the binary nucleation in the ethanol-water system. Although this subject is outside our present scope, we refer to nozzle experiments discussed by Clumpner (1970) and Wegener et al. (1972), and recent shock tube work by Wu and Belle (1974).

b) Experiment and Theory for the Critical Supersaturation.

This final section will be concerned with quantitative comparisons of computed and observed critical supersaturation. However, at first a remark on the accuracy of such comparisons is required. We recall that

* Stein and Armstrong (1973) show that e.g. H₂O clusters in a molecular beam exhibit a diamond cubic structure. However, in these experiments at extreme cooling rates (see Section 4c), the internal degrees of freedom and the rotational mode may well have been "frozen" at the state in the supply. Thus a comparison with the conditions discussed here is not possible.

depending on the latent heat a certain value of Γ the condensate mass fraction is detectable by gasdynamic methods. Consequently values of Γ in the theory, see Eq. (5.26) or empirically, see Eq. (6.1) are matched at this point of departure from isentropic flow. In conjunction with an error analysis of all experimental uncertainties, it is possible to determine the resulting error in the measured nucleation rate. Such an analysis was made for ethanol condensation in a steady nozzle flow (Clumpner 1970). Here the detectable minimum mass fraction is larger than that for water owing to the lower latent heat and therefore the errors may be larger leading to a conservative result. Typically, a pressure deviation from the isentrope of about four times the experimental error leads to a detection of a mass fraction of $g \leq 10^{-3}$. The result of the analysis reveals that at the onset location of condensation in the nozzle in a typical ethanol/air

experiment (e.g. Fig. 6.1), the nucleation rate can be determined within about $\pm 20\%$. Somewhat better values are to be expected for water where the higher latent heat permits the detection of smaller amounts of condensate. However, the much higher critical saturation rates (higher surface tension!) lead to a greater temperature sensitivity in the determination of the saturation pressure. At any rate, we may safely state that nucleation rates can generally be measured by gasdynamic methods within a factor of ten. This value is very much smaller than that of the uncertainties in the available theories, uncertainties in J based on uncertainties in σ_∞ , etc. The experiment of Fig. 6.1 has been recomputed by the simultaneous variation of surface tension and the replacement factor in Eq. (5.26) with the result shown in Fig. 6.8. Each point on the curve shown thus gives a combination of values of σ/σ_∞ and q_{rep}^* which is compatible with the experimental results at the onset of condensation. For $\sigma = \sigma_\infty$, we find $q_{\text{rep}}^* \sim 10^{14}$ assuming as before that the two other partition functions are known from Eqs. (5.26) and (5.27). This value of q_{rep}^* roughly

corresponds to the ideas initially advanced by Kuhrt (1952), and by Dunning (1965) leading to "low" values of Γ in contrast to the work of Lothe and Pound (1966). Plotting the main terms in the nucleation rate equation during the course of the entire condensation zone of Fig. 6.1 we find Fig. 6.9. Only the classical exponential term, here determined for $\sigma = \sigma_{\infty}$, varies dramatically during the expansion. The factor Γ of Eq. (5.26) computed with the Dunning model for q^*_{rep} agrees well with the experiment. Such graphs permit detailed comparisons with the theory not offered by other experimental techniques. In particular, work of this kind ought to be extended to other substances with other properties.

Tables 6.2 and 6.3 finally give results from theory and experiment matched at the critical supersaturation. The non-isothermal theory and the isothermal expression are compared for pure vapor expansions in Table 6.2. In Table 6.3, only the isothermal expressions are used since the condensing vapors were expanded in an excess of carrier gas.* However, once condensation was observed at

* We recall the previous observations on the small effect of the nature of the carrier gas on the onset of condensation.

AD-A036 350

YALE UNIV NEW HAVEN CONN DEPT OF ENGINEERING AND AP--ETC F/G 20/4
GASDYNAMICS AND HOMOGENEOUS NUCLEATION, (U)
JUN 75 P P WEGENER, B J WU

N00014-67-A-0097-0012

UNCLASSIFIED

31

NL

2 of 2
ADA036350



END

DATE
FILMED
3 - 77

temperatures below the triple point, vapor pressures with respect to the liquid (estimated for supercooled states), or solid phase respectively were computed leading to distinctly different answers. Table 6.1 aids in relating n^* to the values of r^* of Tables 6.2 and 6.3. The tables are self-explanatory and they permit varying interpretations. However, the results shown are believed to be the first comparative data collection uniformly based on identical criteria as discussed in Section 5.

A few observations on the results may be in order. For one, the critical radii of the clusters in the range of $4 < r^* < 11 \text{ \AA}$ are appreciably smaller than those observed in cloud chambers. In the latter experiments lower supersaturation is experienced due to the lower cooling rate in line with the empirical relation Eq. (1.1). The small size of the clusters (see Table 6.1) may invalidate all comparisons with the classical theory and its variants. Moreover, for these small clusters the distinctions between the liquid and solid phase and corresponding property selections become blurred as noted before. In fact it is impossible at present to distinguish a priori if liquid or solid properties apply. A case in point is benzene as noted in lines 1 and 2 of

Table 6.3. Applying solid properties at 60 to 80 C below the triple point leads to a supersaturation similar to that of water. In sharp contrast, the assumption that the condensate is a supercooled liquid yields a nucleation rate of about 10^9 times that of the classical rate, i.e. $\Gamma \sim 10^9$.* Recent experiments by Katz et al. (1975) performed in a diffusion cloud chamber show that the nucleation of benzene above the triple point is well described by the classical theory.

In fact, any experimental result exhibiting a "high" nucleation rate in such comparisons may be subject to the additional criticism that vapor impurities have resulted in binary nucleation. Such nucleation yields a lower critical supersaturation. In fact the highest values of J (or Γ) are seen in Table 6.3 for chloroform in lines 6 to 11 based on nozzle and shock tube experiments performed at MIT and Yale respectively. The highest rate value of nucleation $\Gamma = 10^{22}$, was noted in a shock tube (line 11) whose cooling rate was lower than that of the nozzle experiments lines 6 to 10. The liquid chloroform employed in the experiments at our laboratory (Barschdorff 1972b) contained 0.75% ethanol

as a stabilizer. Apparently the same grade (Russell 1971) was used previously in the MIT nozzle experiments (Dawson et al. 1969) seen recomputed in Table 6.3, lines 6 to 10. Condensation appears roughly at the triple point so that the property problem does not enter in this case. In view of the prior experience with binary nucleation, the chloroform data with ethanol present in the mixture cannot be accepted as examples of homogeneous nucleation. Moreover, recent experiments by Katz (1975) with chloroform using a diffusion cloud chamber showed nucleation rates close to that given by the classical theory. This result was obtained with both the sample containing 0.75% ethanol and a purified sample believed to be free of ethanol. The data on chloroform should therefore be considered inconclusive at present.

In sum, the pure vapor expansions tabulated yield results roughly compatible*with the classical theory of nucleation with "low" values of Γ . Without further defining the meaning of "low" in view of all the uncertainties facing us, the results in Table 6.3 tell us that the substances benzene, ammonia, Freon 11, and carbon tetrachloride yield high rates of nucleation. Careful additional experiments ruling out all possibilities of binary nucleation and the study of other substances will be required to further verify the varying nucleation rates given. It is interesting to note that no results on any substance in either Wilson cloud

* We recall that employing e.g. Volmer's equation (Volmer 1969) which is essentially identical to those of other early investigators and viewing Γ as an adjustment factor as in Eq. (6.1) the classical theory yields $\Gamma = 1$.

chambers or diffusion cloud chambers have yet exhibited the behavior of the materials cited giving "high" values of Γ . It is thus truly remarkable that a theory fraught with such uncertainties provides generally consistent answers on nucleation.

8 ACKNOWLEDGMENT

Continuing discussions on all aspects of this work with Dr. W.J. Dunning of Bristol University, England, are gratefully acknowledged. Dr. G. Gyarmathy of Brown, Boverie and Cie. in Switzerland kindly provided the original data and additional unpublished information concerning his high pressure steam condensation work. The research at our own laboratory has enjoyed the support of the Power Program of the United States Office of Naval Research. We are much indebted to this agency and in particular we wish to express our gratitude to Dr. Ralph Roberts who directed the Power Program until the end of 1974, and who contributed in many ways to this work.

LIST OF SYMBOLS

A	Nozzle cross-sectional area.
a	Speed of sound, Eq. (2.10).
b	Eq. (5.29).
c	Wave speed, Eq. (2.37); also specific heat, Eq. (5.10).
c_p	Specific heat at constant pressure.
c_v	Specific heat at constant volume.
D, De	Impingement and evaporation rates, respectively, Eqs. (5.33), (5.34).
d	Eq. (5.30).
e	Internal energy.
f(r)	Size distribution function.
g	Condensate mass fraction.
h	Enthalpy; also nozzle height, Eqs. (2.33), (2.34); also Planck's constant, Eq. (5.26).
I	Moment of inertia.
J	Nucleation rate.
K	$[= (\gamma+1)/2(\gamma-1)]$.
k	Boltzmann's constant.
Kn	Knudsen number, Eq. (2.3).
L	Latent heat of condensation.
l	Characteristic length.
M	Mach number, Eq. (2.2).
m	Molecular mass ($= \mu/N_A$); or index of reflection.
N	Number density of droplets.
n	Number of molecules in a cluster.

N_A	Avogadro's number.
p	Pressure.
Pr	Prandtl number, Eq. (3.13).
\dot{Q}	Mass flow rate through a nozzle, Eq. (2.13).
q	Heat addition to unit mass of the flow.
q_{rep}	Replacement factor, Eq. (5.26).
R	Molar gas constant; also radius of curvature of nozzle contour, Eqs. (2.33), (2.34).
r	Droplet radius.
Re	Reynolds number, Eq. (2.1).
s	Entropy; or saturation ratio ($= p_v/p_\infty$).
T	Temperature.
t	Time.
u	Velocity.
v	Molecular volume.
x	Spatial coordinate.
α	Mass accommodation coefficient.
α'	Effective condensation coefficient, Eq. (5.35).
Γ	Eqs. (5.25) and (6.1).
γ	Ratio of specific heats, Eq. (2.9) ($= c_p/c_v$).
η	Viscosity.
κ	Thermal conductivity.
λ	Mean free path; also wavelength.
μ	Molecular weight.
ν	kinematic viscosity ($= \eta/\rho$).

ξ	Thermal accommodation coefficient.
ρ	Density.
ρ'_c	Density of condensate referred to the volume of the gas phase.
σ	Surface tension.
τ	Relaxation time.
Φ	Relative humidity = $(p_v/p_\infty) \times 100\%$.
ϕ	Progress variable.
Ψ	Eq. (3.3).
ω	Mass fraction.

Subscripts and superscripts.

ad	adiabatic.
c	condensate.
cl	classical.
crit	Refers to critical point.
d	Refers to droplet.
e	Equilibrium.
exp	Experimental.
f	Frozen flow.
i	Inert carrier gas.
iso	Isothermal.
noniso	Nonisothermal.
r	Refersto droplets with radius r.
s	Shock; also for saturation.
T	Refers to properties of two-phase medium.

- th Theoretical.
- v Vapor.
- o Stagnation conditions; also for conditions in the supply.
- 01 Supply conditions.
- 1,2,3,4 Refersto shock tube flow regions, Fig. 2.2.
- ∞ Refers to bulk properties.
- * Sonic conditions at nozzle throat; or for critical clusters.

REFERENCES

- Anderson, J.B., Andres, R.P., Fenn, J.B., and Maise, G. (1966) Proc. 4th Symp. on Rarefied Gas Dynamics, (ed. J.H. deLeeuw), II, 106, Academic Press, N.Y.
- Andres, R.P. and Boudart, M. (1965) *J. Chem. Phys.* 42, 2057.
- Arthur, P.D., (1952) Ph.D. Thesis, Cal. Inst. of Tech., Pasadena, Calif.
- Barschdorff, D. (1970) Presented 3rd Intern. Conf. on Rain Erosion and Associated Phenomena, England, August.
- Barschdorff, D. (1971) *Forsch. Ing.-Wes.* 37, 146.
- Barschdorff, D., Dunning, W.J., Wegener, P.P. and Wu, B.J.C., (1972) *Nature-Physical Science* 240, 166.
- Barschdorff, D. (1972a) Proc. Intern. Workshop on Nucleation, (Eds. C.S. Kiang and V.A. Mohnen), April, Clark College, Atlanta, Ga.
- Barschdorff, D. (1972b) Unpublished data, Yale University, New Haven, Conn.
- Barschdorff, D. and Ludwig, A. (1972) Private communication, Univ. of Karlsruhe, Karlsruhe, Germany.
- Barschdorff, D., Hausman, G. and Ludwig, A. (1974) Proc. Conf. on Steam Turbines of Great Output, Polish Academy of Sciences, Inst. of Fluid Flow Machinery, Gdansk, Poland, Sept.
- Barschdorff, D. (1975) *Phys. Fluids* (in press).
- Becker, E. (1972) Ann. Rev. Fluid Mech. 4, 155, Annual Reviews Inc., Palo Alto, Calif.
- Becker, E.W. and Henkes, W. (1956) *Z. Physik* 146, 320.
- Becker, R. and Döring, W. (1935) *Ann. Physik* 24, 719.

- Benson, G.C. and Shuttleworth, R. (1951) *J. Chem. Phys.* 19, 130.
- Binnie, A.M. and Woods, M.W. (1938) *Proc. Inst. Mech. Engineers* 138, 229.
- Binnie, A.M. and Green, J.R. (1943) *Proc. Roy. Soc. (London)* A181, 134.
- Bray, K.N.C. (1959) *J. Fluid Mech.* 6, 1.
- Bray, K.N.C. (1970) *Nonequilibrium Flows*, (Ed. P.P. Wegener) Part II, Chap. 3. Marcel Dekker, N.Y.
- Broer, L.J.F. (1951) *Appl. Sci. Res.* A2, 447.
- Buckle, E.R. and Pouring, A.A. (1965) *Nature* 208, 367.
- Campbell, B.A. and Bakhtar, F. (1973) *Heat and Fluid Flow*, 3, 51, *Inst. Mech. Engineers*, London.
- Chmielewski, T. and Sherman, P.M. (1970) *AIAA J.* 8, 789.
- Chu, B.T. (1958) *Heat Transfer and Fluid Mechanics Institute - Preprints of Papers*, p.80. Stanford University Press.
- Clumpner, J.A. (1970) Ph.D. Thesis, Yale University, New Haven, Conn.
- Clumpner, J.A. (1971) *J. Chem. Phys.* 55, 5042.
- Courtney, W.G. (1962) *J. Chem. Phys.* 36, 2018.
- Dawson, D.B., Willson, E.J., Hill, P.G. and Russell, K.C. (1969) *J. Chem. Phys.* 51, 5389.
- Deych, M. Ye. and Filipov, G.A. (1968) *The Gasdynamics of Two-Phase Media*, Translated by Foreign Technology Division, Wright-Patterson AFB, Ohio (1970) Available from NTIS, ref. no. AD701975.
- Deych, M. Ye., Stepanchuk, V.F. and Saltanov, G.A. (1969a) *Heat Trans. - Soviet Res.* 1, no.2, 106.

- Deych, M.Ye., Saltanov, G.A., Stepanchuk, V.F. and Orlova, M.
(1969b) Heat Trans. - Soviet Res. 1, no.2, 135.
- Duff, K.M. and Hill, P.G. (1966) Proc. 1966 Heat Trans. and
Fluid Mechanics Instit. p.268. (Eds. M.A. Saad, J.A.
Miller) Stanford Univ. Press.
- Dunning, W.J. (1960) Discussions of The Faraday Society, No.30.
- Dunning, W.J. (1965) Colloques Internationaux du Centre
National de la Recherche Scientifique, No. 152, p.369,
CNRS, Paris.
- Dunning, W.J. (1969) Nucleation (Ed. A.C. Zettlemoyer) Chap.1.
Marcel Dekker, N.Y.
- Eber, G. and Gruenewald, K.H. (1941/42) Private communication.
- Feder, J., Russell, K.C., Lothe, J. and Pound G. (1966)
Advances in Physics 15, 111.
- Frankel, J. (1946) Kinetic Theory of Liquids, Chap. VII, p. 366
Oxford Univ. Press, N.Y.
- Glass, I.I. and Patterson, G.N. (1955) J. Aeronautical Sci.
22, 73.
- Griffin, J.L. and Sherman, P.M. (1965) AIAA J. 3, 1813.
- Gyarmathy, G. (1963) ZAMP 14, 280.
- Gyarmathy, G. and Meyer, H. (1965) VDI-Forschungsheft 508,
VDI-Verlag GMBH Düsseldorf.
- Gyarmathy, G., Burkhard, H-P., Lesch, F. and Siegenthaler, A.
(1973) Inst. Mech. Engrs. (London) Conf. Publ. 3
- Hagena, O.F. (1974) Molecular Beams and Low Density Gasdynamics,
(Ed. P.P. Wegener) Chap.2, Marcel Dekker, N.Y.
- Hermann, R. (1942) Luftfahrtforschung 19, 201.
- Hill, P.G., Witting, H. and Demetri, E.P. (1963) Transactions
of the ASME 85, Ser. C, J. Heat Transfer 303.

- Hill, P.G. (1966) *J. Fluid Mech.* 25, 593.
- Homer, J.B. and Hurle, I.R. (1972) *Proc. Roy. Soc. (London)* A.327, 61.
- Homer, J.B., Hurle, I.R. and Swain, P.J. (1971) *Nature* 229, 251.
- Jaeger, H.L., Willson, E.J., Hill, P.G. and Russell, K.C. (1969) *J. Chem. Phys.* 51, 5380.
- Kantrowitz, A. (1951) *J. Chem. Phys.* 19, 1097.
- Kassner, J.L. and Schmitt, R.J. (1966) *J. Chem. Phys.* 44, 4166.
- Katz, J.L. (1975) Abstract of Papers, 169 National Meeting, American Chemical Society Publication, April.
- Katz, J.L., Scoppa, C.J., Kumar, N.G. and Mirabel, P. (1975) *J. Chem. Phys.* 62, 448.
- Kirkwood, J.G. and Buff, F.P. (1949) *J. Chem. Phys.* 17, 338.
- Knudsen, M. (1915) *Ann. der Physik* 47, 697.
- Kuhrt, F. (1952a) *Z. Physik* 131, 185.
- Kuhrt, F. (1952b) *Z. Physik* 131, 205.
- Kung, R.T.V. and Bauer, S.H. (1971) Proc. 8th Intern. Shock Tube Symposium, London (Eds. J.L. Stollery, A.G. Gaydon, P.R. Owen) Paper #61, July, Chapman & Hall, London.
- Lednovich, S.L. (1974) Ph.D. Thesis, Yale University, New Haven, Conn.
- Lee, C.F. (1974) Private communication, Yale University, New Haven, Conn.
- Lothe, J. and Pound G.M. (1962) *J. Chem. Phys.* 36, 2080.

- Lothe, J. and Pound, G.M. (1966) *J. Chem. Phys.* 45, 630.
- Lothe, J. and Pound, G.M. (1969) Nucleation, (Ed. A.C. Zettlemoyer) Chap. 3, 109, Marcel Dekker, N.Y.
- Lukasiewicz, J. and Royle, J.K. (1948) *Aero. Res. Counc.(GB) Repts. & Mem.* #2563.
- Marble, F.E. (1969) *Astronautica Acta* 14, 585.
- Mills, A.F. and Seban, R.A. (1967) *Int. J. Heat Mass Transf.* 10, 1815.
- Oriani, R.A. and Sundquist, B.E. (1963) *J. Chem. Phys.* 38, 2082.
- Oswatitsch, K. (1941) Jahrbuch der deutschen Luftfahrtforschung, I, 692.
- Oswatitsch, K. (1942) *Z. Angewandte Mathematik and Mechanik* 22, 1.
- Paul, B. (1962) *ARS J.* 32, 1321.
- Petty, D.G., Blythe, P.A. and Shih, C.J., AD-756471, NTIS, Springfield, Va. 22151.
- Pouring, A.A. (1963) Ph.D. Thesis, Yale University, New Haven, Conn.
- Prandtl, L. (1935) *l.c. Volta Congress.*
- Puzyrewski, R. (1967) *Int. J. Heat Mass Trans.* 10, 1717.
- Puzyrewski, R. (1969) *Inst. of Fluid Flow Machinery, Polish Academy of Sciences, Gdansk.*
- Reiss, H. (1970) *J. Statistical Phys.* 2, 83.
- Roberts, R. (1969) Report No.97, MIT, Gas Turbine Lab., Cambridge, Mass.
- Russell, K.C. (1971) Private communication, Mass. Inst. Tech. Cambridge, Mass.

- Smith, L.T. (1971) AIAA J. 9, 2035.
- Stein, G.D. (1967) Ph.D. Thesis, Yale University, New Haven, Conn.
- Stein, G.D. (1969a) J. Chem. Phys. 51, 938.
- Stein, G.D. (1969b) Rev. Sci. Instr. 40, 1058.
- Stein, G.D. and Armstrong, J.A. (1973) J. Chem. Phys. 58, 1999.
- Stein, G.D. and Moses, C.A. (1972) J. Colloid and Interface Sci. 39, 504.
- Stever, H.G. (1958) Fundamentals of Gas Dynamics, (Ed.H.W. Emmons) Princeton Univ. Press, p. 526.
- Stodola, A. (1927) Steam and Gas Turbines, McGraw-Hill, N.Y.
- Tolman, R.C. (1949) J. Chem. Phys. 17, 333.
- Volmer, M. (1939) Kinetik der Phasenbildung, Steinkopff, Dresden und Leipzig.
- Volta, Reale Accademia D'Italia, Fondazione Allesandro Volta.
Atti dei Convegni 5, Le Alte Velocita in Aviazione,
(1935) - XIII Roma, First ed. 1936-XIV, Second ed.
1940-XIX.
- Wegener, P.P. and Lundquist, G. (1951) J. Appl. Phys. 22, 233.
- Wegener, P.P. (1954) J. Appl. Phys. 25, 1485.
- Wegener, P.P. and Mack L. (1958) Advances in Applied Mechanics,
V, p. 307, Academic Press, Inc., N.Y.
- Wegener, P.P. (1964) Heterogeneous Combustion, (Vol. 15,
Progress in Astronautics and Aeronautics) ed. H.G.
Wolfhard, I. Glassman and L. Green, Academic Press,
Inc., N.Y., p. 701.

- Wegener, P.P. and Pouring, A.A. (1964) *Phys. Fluids* 7, 131.
- Wegener, P.P. (1966) Feature, *Chem. & Eng. News* 44, 76.
- Wegener, P.P. and Parlange, J.-Y. (1967) 7th AGARD Coll. on Recent Advances in Aerothermochemistry, Oslo (Norway), May, AGARD Conf. Proc. No.12, Vol. 2, p. 607 (ed. I. Glassman).
- Wegener, P.P. (1969) Nonequilibrium Flows (ed. P.P. Wegener). Part 1, Chap.4, p. 163. Marcel Dekker, N.Y. N.Y.
- Wegener, P.P. and Stein, G.D. (1969) 12th Symposium (Intern.) on Combustion, The Combustion Institute, Mono of Maryland, Inc., p. 1183.
- Wegener, P.P. and Parlange, J.-Y. (1970) *Die Naturwissenschaften*, 57, 525.
- Wegener, P.P., Clumpner, J.A. and Wu, B.J.C. (1972) *Phys. Fluids* 15, 1869.
- Wegener, P.P. and Cagliostro, D. (1973) *Comb. Sci. and Tech.* 6, 269.
- Wegener, P.P. (1975) *Acta Mechanica* 21, 65.
- Wilson, C.T.R. (1897) *Trans. Roy. Soc. (London)*, A189, 265.
- Wu, B.J.C. (1972) Ph.D. Thesis, Yale University, New Haven, Conn.
- Wu, B.J.C. (1974) AD775257 Available from NTIS, Springfield, Va.
- Wu, B.J.C. and Belle, K.C. (1974) *Bull. APS* II 19, 1150.
- Yellot, J.L. and Holland, C.K. (1937) *Trans. ASME* 59, 171.

APPENDIX 1

Compressible Flow Table. Perfect Gas, $\gamma = 7/5 = 1.400$.

M	p/p_0	ρ/ρ_0	T/T_0	A/A^*	u/a^*
0.0	1.0000	1.0000	1.0000	∞	0.0000
0.2	0.9725	0.9803	0.9921	2.964	0.2182
0.4	0.8956	0.9243	0.9690	1.590	0.4313
0.6	0.7840	0.8405	0.9328	1.188	0.6348
0.8	0.6560	0.7400	0.8865	1.038	0.8251
1.0	0.5283	0.6339	0.8333	1.000	1.0000
1.2	0.4124	0.5311	0.7764	1.030	1.1583
1.4	0.3142	0.4374	0.7184	1.115	1.2999
1.6	0.2353	0.3557	0.6614	1.250	1.4254
1.8	0.1740	0.2868	0.6068	1.439	1.5360
2.0	0.1278	0.2300	0.5556	1.688	1.6330
2.2	0.09352	0.1841	0.5081	2.005	1.7179
2.4	0.06840	0.1472	0.4647	2.403	1.7922
2.6	0.05012	0.1179	0.4252	2.896	1.8571
2.8	0.03685	0.09463	0.3894	3.500	1.9140
3.0	0.02722	0.07623	0.3571	4.235	1.9640
3.5	0.01311	0.04523	0.2899	6.790	2.0642
4.0	0.006586	0.02766	0.2381	10.72	2.1381
4.5	0.003455	0.01745	0.1980	16.56	2.1936
5.0	0.001890	0.01134	0.1667	25.00	2.2361
10.0	0.0000236	0.000495	0.04762	535.9	2.3905

APPENDIX 2

Condensation Studies in Compressible Flow Systems.

A chronological list of publications on homogeneous nucleation in flow systems is assembled. These papers contain experimental data and/or they are based on the authors' own or other experimental results. Investigations motivated by the understanding of the physics of homogeneous nucleation as well as those in which technological problems inspired the studies are both listed. No claim is made for completeness. In fact owing to the uncertainties attached to many "air" condensation studies in hypersonic wind tunnels (i.e. wind tunnels for $M \gg 1$), few experiments on "air" condensation are included. Moreover the many low speed condensation studies on two-phase equilibrium flows, studies of purely diabatic flow and of unsteady nozzle flow with condensation are omitted. Finally, the field of clustering in molecular beams (see Section 4c) is completely omitted; it was recently covered extensively by Hagena (1974), and it falls outside the scope of the current article.

1866

Hirn, G.A. and Cazin, A., "Expériences sur la détente de la vapeur d'eau surchauffée," Comptes rendus de l'academie française, 63, 1144.

1927

Stodola, A., Steam and Gas Turbines, Vols. I and II, Translated from the 6th German Edition by L.C. Loewenstein, McGraw-Hill, N.Y., Sections 41 and 178-180.

1934

Yellot, J.L., "Supersaturated Steam," Trans. ASME 56, 411.

1935

Volta, Reale Accademia D'Italia, Fondazione Alessandro Volta, Atti dei Convegni 5, Le Alte Velocita in Aviazione, 30 Sept. to 6 Oct. 1935 - XIII Roma, First Edition 1936-XIV, Second Edition 1940-XIX.

1936

Rettaliata, J.T., "Undercooling in Steam Nozzles," Trans. ASME 58, 599.

1937

Yellot, J.L. and Holland, C.K., "The Condensation of Flowing Steam - Part I, Condensation in Diverging Nozzles," Trans. ASME 59, 171.

1938

Binnie, A.M. and Woods, M.W., "The Pressure Distribution in a Convergent-Divergent Steam Nozzle," Proc. Inst. Mech. Engineers, 138, 229.

1941

Oswatitsch, K., Die Nebelbildung in Windkanälen und ihr Einfluss auf Modellversuche," Jahrbuch der deutschen Luftfahrtforschung, I, 692.

Eber, G. and Gruenewald, K.H., Schlieren-photography of Condensation Disturbances in the 40 x 40 cm Peenemünde Supersonic Wind Tunnels. Private communication, also Wegener and Mack (1958).

1942

Hermann, R., "Der Kondensationsstoss in Überschall-Windkanaldüsen," Luftfahrtforschung, 19, 201.

Heybey, W., "Analytische Behandlung des geraden Kondensationsstosses," Heeresversuchsstelle Peenemuende, Archiv Nr. 66/72, Also NACA TM 1174 (1947).

Oswatitsch, K., "Kondensationserscheinungen in Überschalldüsen," Zeitschrift für angewandte Mathematik and Mechanik, 22, 1.

Oswatitsch, K., Kondensationsstösse in Lavalldüsen. Z. VDI, 86, 702.

1943

Binnie, A.M. and Green, J.R., "An Electrical Detector of Condensation in High Velocity Steam," Proc. Roy. Soc. (London) A181, 134.

1945

Taylor, G.I., "Pitot Pressures in Moist Air," Gt. Brit. Aeronautical Research Council, Reports & Memoranda No. 2248, 29 Jan. 1945, Re-Published 1955, London.

1946

Charyk, J.V., "Condensation Phenomena in Supersonic Flows," Doctoral Dissertation, California Institute of Technology, Pasadena, California.

1948

Lukasiewicz, J. and Royle, J.K., "Effects of Air Humidity in Supersonic Wind Tunnels," Aeronautical Research Council Reports and Memoranda, No. 2563.

Wegener, P.P., "On the Experimental Investigation of Hypersonic Flow," U.S. Naval Ord. Lab., White Oak, Md. Mem. #9629.

1949

Head, R.M., "Investigations of Spontaneous Condensation Phenomena," Doctoral Dissertation, California Institute of Technology, Pasadena, California.

Wegener, P.P., "Experiments on the Influence of Temperature Gradients and Humidity on Condensation Shocks in Supersonic Wind Tunnels," Phys. Rev. 76, 883, (ABSTRACT).

1950

Becker, J.V., "Results of Recent Hypersonic and Unsteady Flow Research at the Langley Aeronautical Laboratory," J. Appl. Phys. 21, 619.

1951

Burgess, W.C. and Seashore, F.L., "Criteria for Condensation-free Flow in Supersonic Tunnels," Natl. Adv. Comm. Aero. Tech. Note. #2518.

Durbin, E.J., "Optical Methods Involving Light Scattering for Measuring Size and Concentration of Condensation Particles in Supercooled Hypersonic Flow," Nat. Adv. Comm. Aero. Tech. Note #2441.

Kantrowitz, A., "Nucleation in Very Rapid Vapor Expansions," J. Chem. Phys., 19, 1097.

Probstein, R.F., "Time Lag in Self-nucleation of a Supersaturated Vapor," J. Chem. Phys., 19, 619.

1951 - continued

Stever, H.G. and Rathbun, K.C., "Theoretical and Experimental Investigation of Condensation of Air in Hypersonic Wind Tunnels," Nat. Adv. Comm. Aero., Tech. Note #2559.

Wegener, P.P., "Summary of Recent Experimental Investigations in the N.O.L. Hyperballistics Wind Tunnel," J. Aero. Sci., 18, 665.

Wegener, P.P. and Lundquist, G., "Condensation of Water Vapor in the Shock Tube Below 150°K.," J. Appl. Phys. 22, 233.

Wegener, P.P., Reed, S., Stollenwerk, E., and Lundquist, G., "Air Condensation in Hypersonic Flow," J. Appl. Phys., 22, 1077.

1952

Arthur, P.D., "Effects of Impurities on the Supersaturation of Nitrogen in a Hypersonic Wind Tunnel," Doctoral Dissertation, California Institute of Technology, Pasadena, Calif.

Buhler, R.D., "Condensation of Air Components in Hypersonic Wind Tunnels - Theoretical Calculations and Comparison with Experiment," Doctoral Dissertation, California Institute of Technology, Pasadena, California.

Faro, I.D., Small, T.R., and Hill, F.K., "The Supersaturation of Nitrogen in a Hypersonic Wind Tunnel," J. Appl. Phys. 23, 40.

Hansen, C.F. and Nothwang, G.J., "Condensation of Air in Supersonic Wind Tunnels and its Effects on Flow About Models," Nat. Adv. Comm. Aero., Technical Note #2690.

Reed, S.J., Jr., "Some Examples of Weak Detonations," J. Chem. Phys., 20, 1823.

Willmarth, W.W. and Nagamatsu, H.T., "The Condensation of Nitrogen in a Hypersonic Nozzle," J. Appl. Phys. 23, 1089.

1954

McLellan, C.H. and Williams, T.W., "Liquefaction of Air in the Langley 11-inch Hypersonic Tunnel," Nat. Adv. Comm. Aero., Technical Note #3302.

Wakeshima, H., "Time Lag in Self-Nucleation," J. Chem. Phys., 22, 1614.

Wegener, P.P., "Water Vapor Condensation Process in Supersonic Nozzles," J. Appl. Phys., 25, 1485.

1955

Glass, I.I. and Patterson, G.N., "A Theoretical and Experimental Study of Shock Tube Flows," J. Aeronaut. Sci. 22, 73.

Heybey, W.H. and Reed, S.G., Jr., "Weak Detonations and Condensation Shocks," J. Appl. Phys., 26, 969.

Wakeshima, H., "Spontaneous Condensation in a Supersonic Flow of Humid Air," J. Phys. Soc. Japan, 10, 141.

1956

Cawthon, J.A., "Water Vapor Condensation Effects in the Ordnance Aerophysics Laboratory," Supersonic Wind Tunnel Rept. #340-1, Ord. Aerophys. Lab., Daingerfield, Texas.

Smith, W.O., "Nucleation and Condensation of Supersaturated Steam during Steady Flow Processes," Doctoral Dissertation, Purdue University, Lafayette, Indiana.

Smolderen, J.J., "Condensation Effects and Air Drying Systems for Supersonic Wind Tunnels," AGARDograph #17, NATO, Paris.

1958

Stever, H.G., "Condensation Phenomena in High Speed Flows," in Fundamentals of Gas Dynamics, Edited by H.W. Emmons, Princeton Univ. Press, pp. 526-573.

1958 - continued

Wegener, P.P. and Mack, L., "Condensation in Supersonic and Hypersonic Wind Tunnels," Advances in Applied Mechanics, Vol.V, Academic Press, Inc., New York, pp. 307-447.

1959

Wegener, P.P. and Mack, L., "Comments on Condensation in Nozzles," J. Appl. Phys. 30, 1624.

1960

Dunning, W.J., "Nucleation Processes and Aerosol Formation," in The Physical Chemistry of Aerosols, Discussions of the Faraday Society, No.30, p.9.

1961

Courtney, W.C., "Recent Advances in Condensation and Evaporation," ARS Journal 31, 751.

Goglia, G.L., and Van Wylen, G.J., "Experimental Determination of Limits of Supersaturation of Nitrogen Vapor Expanding in a Nozzle," Trans. ASME 83, Ser.C, 27, (J. Heat Transfer).

1962

Schmidt, B., "Beobachtungen über das Verhalten der durch Wasserdampfkondensation ausgelösten Störungen in einer Überschall-Windkanaldüse, Doctoral Dissertation, Univ. Karlsruhe, Karlsruhe, Germany.

1963

Clark, D.R., "On the Flow in the Nozzle of a Condensing Diatomic Vapour," College of Aeronautics Report #165, Cranfield, England.

Gyarmathy, G., "Kondensationsstoss-Diagramme für Wasserdampfströmungen," Forsch. Ing.-Wes., 29, 106.

1963 - continued

Hill, P.G., Witting, H., and Demetri, E.P., "Condensation of Metal Vapors during Rapid Expansion," Trans. ASME, 85, Ser.C, 303, (J. Heat Transfer).

Pouring, A.A., "An Experimental and Analytical Investigation of Homogeneous Condensation of Water Vapor in Air during Rapid Expansion," Doctoral Dissertation, Yale Univ., New Haven, Conn.

1964

Bartlmä, F., "Ebene Überschallströmung mit Relaxation," Proceedings of the Eleventh International Congress of Applied Mechanics, Munich, Germany, Springer-Verlag, N.Y. published 1966, p. 1056.

Duff, K.M., "Condensation of Carbon Dioxide in Supersonic Nozzles," Gas Turbine Lab., Massachusetts Institute of Technology, Report #76.

Dunning, W.J., "Experimental Methods for the Study of Nucleation and Condensation," p.739 in Heterogeneous Combustion, (Vol.15, Progress in Astronautics and Aeronautics) Ed. H.G. Wolfhard, I. Glassman and L. Green, Academic Press, N.Y.

Griffith, B.J., Deskins, H.E., and Little, H.R., "Condensation in Hotshot Tunnels," Arnold Eng. Develop. Center, Arnold Air Force Station, Tenn. AEDC-TDR-64-35.

Thomann, H., "Determination of the Size of Ice Crystals Formed During Condensation of Water in Wind Tunnels and of Their Effect on Boundary Layers," The Aeronautical Research Institute of Sweden, Report 101.

Wegener, P.P., "Condensation Phenomena in Nozzles," p. 701 in Heterogeneous Combustion, (Vol.15, Progress in astronautics and Aeronautics) Ed. H.G. Wolfhard, I. Glassman and L. Green, Academic Press, New York.

1964 - continued

Wegener, P.P. and Pouring, A.A., "Experiments on Condensation of Water Vapor by Homogeneous Nucleation in Nozzles," Phys. Fl. 7, 131.

1965

Buckle, E.R. and Pouring, A.A., "Effects of Seeding on the Condensation of Atmospheric Moisture in Nozzles," Nature, 208, 367.

Daum, F.L. and Gyarmathy, G., "Air Condensation in Rapidly Expanding Hypersonic Flow," XVI International Astronautical Congress, Athens, Greece.

Griffin, J.L. and Sherman, P.M., "Computer Analysis of Condensation in Highly Expanded Flows," AIAA J. 3, 1813.

Gyarmathy, G and Meyer, H., "Spontane Kondensation," VDI-Forschungsheft 508, VDI-Verlag GMBH Düsseldorf.

Harding, L.J., "A Digital Computer Program for Condensation in Expanding One-Component Flows," ARL Report 65-58, Aerospace Research Laboratories, Wright Patterson AFB, Ohio.

Kremmer, M. and Okorounmu, O. "Condensation of Ammonia Vapor During Rapid Expansion," Gas Turbine Lab., Mass. Institute of Technology, Report No. 79.

Walton, A.G. (Editor) International Symposium on Nucleation - Abstract of the Proceedings April 7-9, Case Institute of Technology, Cleveland, Ohio. See contributions by P.P. Wegener, "Condensation of Water Vapor by Homogeneous Nucleation in a Supersonic Nozzle," p.14; and by P.G. Hill, "Homogeneous Nucleation and Condensation of Water Vapor, Carbon Dioxide, and Ammonia in Supersonic Nozzles," p.16.

1966

Duff, K.M., "Non-equilibrium Condensation of Carbon Dioxide in Supersonic Nozzles," Gas Turbine Lab., Mass. Institute of Technology, Report No. 84.

1966 - continued

Duff, K.M. and Hill, P.G., Condensation of Carbon Dioxide in Supersonic Nozzles, Proc. of the 1966 Heat Transfer and Fluid Mechanics Institute, (Ed. M.A. Saad, J.A. Miller) Stanford Univ. Press, p. 268.

Hill, P.G., "Condensation of Water Vapor during Supersonic Expansion in Nozzles," J. Fluid Mech. 25, 593.

Jaeger, H.L., "Condensation of Supersaturated Ammonia and Water Vapor in Supersonic Nozzles," Gas Turbine Lab., Mass. Institute of Technology, Report No.86.

Merritt, G.E. and Weatherston, R.C., "Condensation of Mercury Vapor and Drop Growth Processes in a Nitrogen Flow," AIAA Paper No. 66-85, AIAA 3rd Aerospace Sciences Meeting, New York, N.Y.

Wegener, P.P., "Gasdynamics, Impact of Chemistry," Feature Article, Chem. & Eng. News, 44, 76.

1967

Barschdorff, D., "Kurzzeitfeuchtemessung und ihre Anwendung bei Kondensationserscheinungen in Lavaldüsen," Strömungsmechanik und Strömungsmaschinen, 6, 18. Verlag Braun, Karlsruhe, Germany.

Dawson, D.B., "Condensation of Supersaturated Organic Vapors in a Supersonic Nozzle," Gas Turbine Lab., Report 90, Mass. Institute of Technology, Cambridge, Mass.

Merritt, G.E. and Weatherston, R.C., "Condensation of Mercury Vapor and Drop Growth Processes in a Nitrogen Flow," AIAA J. 5, 721.

Podvidz, G.L., "Supersaturation and Condensation Shock During Flow of Potassium Vapor," Translation, Teplofizika Vysokikh Temperatur, 5, 121, NASA TT F-11, 182.

1967 - continued

Pouring, A.A., (Editor) Symposium on Nucleation Phenomena in Gas Dynamics - Abstract of the Proceedings. 7-8 Dec., U.S. Naval Academy, Annapolis, Maryland. See contributions by P.P. Wegener, "Light Scattering Measurements of Condensation in Supersonic Flow," p.1; by R.C. Weatherston, "Hypersonic Condensation," p.15; by P.M. Sherman and D.D. McBride, "Sampling and Pressure Measurements in Two-Component Two-Phase Flow," p.16; and by P.G. Hill and K.C. Russell, "Experimental Data on Condensation of Several Vapors in Nozzles," p.24.

Sherman, P.M., McBride, D.D., and Oktay, E., "Condensation in a Rapidly Expanding Metal Vapor-Inert Gas Mixture," Aerospace Research Laboratories, ARL 67-0071.

Stein, G.D., "Condensation of Ice Clusters by Homogeneous Nucleation from the Vapor Phase," Doctoral Dissertation, Yale Univ., New Haven, Conn.

Stein, G.D., and Wegener, P.P., "Experiments on the Number of Particles Formed by Homogeneous Nucleation in the Vapor Phase," J. Chem. Phys. 46, 3685.

Wegener, P.P. and Parlange, J.-Y., "Nonequilibrium Nozzle Flow with Condensation," 7th AGARD Coll. on Recent Advances in Aerothermochemistry, Oslo, (Norway) and AGARD Conference Proceedings, No.12, Recent Advances in Aerothermochemistry 2, pp. 607, ed. I. Glassman.

1968

Daum, F.L. and Gyarmathy, G., "Condensation of Air and Nitrogen in Hypersonic Wind Tunnels," AIAA Journal, 6, 458.

1968 - continued

Deych, M. Ye. and Filipov, G.A., "The Gasdynamics of Two-Phase Media," Translated by Foreign Technology Division, Wright Patterson AFB, Ohio, (1970), Available from NTIS, ref. no. AD701975.

Falk, T.J., "Research on Hypersonic Condensation Phenomena in High Temperature Gases, Vol. II, Condensation Experiments in a Shock Tube," ARL-Report 68-0143, Aerospace Research Laboratories, Wright Patterson AFB, Ohio.

Wegener, P.P., "Light Scattering Measurements of Condensation in Supersonic Flow," Abstracts of papers, 155th National Meeting, American Chemical Society Publication, San Francisco, Calif., Abstract H16.

1969

Andres, R.P., "Homogeneous Nucleation in a Vapor," Chapter 2 in Nucleation, ed. A.C. Zettlemoyer, Marcel Dekker, Inc. New York.

Dawson, D.B., Willson, E.J., Hill, P.G. and Russell, K.C., "Nucleation of Supersaturated Vapors in Nozzles," II, C_6H_6 , $CHCl_3$, CCl_3F , and C_2H_5OH ," J. Chem. Phys. 51, 5389.

Deych, M. Ye., Kurshakov, A.V., Saltanov, G.A. and Yatcheni, I.A., "A Study of the Structure of Two-Phase Flow Behind a Condensation Shock in Supersonic Nozzles," Heat Transfer-Soviet Research 1, No.5, 95.

Deych, M. Ye., Saltanov, G.A., Stepanchuk, V.F. and Orlova, M., "Study of Energy Losses in Condensation Discontinuities and Shocks in the Flow of Wet Steam," Heat Transfer-Soviet Research 1, No.2, 135.

1969 - continued

- Deych, M. Ye., Stepanchuk, V.F. and Saltanov, G.A., "Calculation of the Rate of Formation of Condensation Centers in Supercooled Vapor," Heat Transfer-Soviet Research 1, No.2,106.
- Jaeger, H.L., Willson, E.J., Hill, P.G. and Russell, K.C., "Nucleation of Supersaturated Vapors in Nozzles, I, H₂O and NH₃," J. Chem. Phys. 51, 5380.
- Marble, F.E., "Some Gasdynamic Problems in the Flow of Condensing Vapors," Astronautica Acta, 14, 585.
- Mori, Y., Kawada, H. and Hijikata, K., "A Study on Condensation Phenomena in Supersonic Flow," Bull. JSME 12, 927, (English Translation of Abstract), Original paper in JSME Bull. (Japanese Language) 34, 2155.
- Puzyrewski, R., "Theoretical and Experimental Studies on Formation and Growth in Water Drops in LP Steam Turbines," Prace Instytutu Maszyn Przeplywowych Zeszyt 42-44, Session IV A. p. 289.
- Roberts, R., "A Light Scattering Investigation of Droplet Growth in Nozzle Condensation," Gas Turbine Lab. Massachusetts Institute of Technology, Report No. 97.
- Stein, G.D., "Angular and Wavelength Dependence of the Light Scattered from a Cloud of Particles Formed by Homogeneous Nucleation," J. Chem. Phys. 51, 938.
- Sugawara, M. and Oshima, N., "Analysis of Condensation in Supersonic Nozzles," Proceedings of the 12th Symposium (International) on Combustion, p. 1193, Pub. by Combustion Institute, Pittsburgh.
- Wegener, P.P., "Gasdynamics of Expansion Flows with Condensation, and Homogeneous Nucleation of Water Vapor," Chapter 4 of Nonequilibrium Flows, (ed. P.P. Wegener), part 1, p.163, Marcel Dekker, Inc., New York.

1969 - continued

Wegener, P.P., "Dynamics of Particle-Vapor Interaction in Condensing Supersonic Flow," Int. Union of Theor. and Appl. Mechanics, Symposium on Flow of Fluid-Solid Mixtures, Cambridge, England, (ABSTRACT).

Wegener, P.P. and Stein G.D., "Light-Scattering Experiments and Theory of Homogeneous Nucleation in Condensing Supersonic Flow," p. 1183, 12th Symposium (International) on Combustion, The Combustion Institute, Pittsburgh.

1970

Barschdorff, D., "Density Measurement in Steam Flow with a Differential Interferometer," Presented at the III. International Kongress für Photographie und Film in Industrie und Technik, Köln.

Barschdorff, D., "Droplet Formation, Influence of Shock Waves and Instationary Flow Patterns by Condensation Phenomena at Supersonic Speeds," Presented at the Third International Conference on Rain Erosion and Associated Phenomena, Royal Aircraft Establishment, Farnborough, England.

Campbell, B.A. and Bakhtar, F., "Condensation Phenomena in High Speed Flow of Steam." The Institution of Mechanical Engineers, Thermodynamics and Fluid Mechanics Group, Proceedings 185, 25/71, 395. See also formal discussions on this paper by Gyarmathy, G., in the same volume.

Chmielewski, T. and Sherman, P.M., "Effect of Carrier Gas on Homogeneous Condensation in a Supersonic Nozzle," AIAA J. 8, 789.

Clumpner, J.A., "Condensation of Ethyl Alcohol in a Nozzle," Doctoral Dissertation, Yale Univ., New Haven, Conn.

1970 - continued

Gyarmathy, G., and Lesch, F., "Fog Droplet Observations in Laval Nozzles and in an Experimental Turbine," Proc. Inst. Mech. Engineers 184, part 3G (III), Paper 12.

Petr, V., "Measurement of an Average Size and Number of Droplets During Spontaneous Condensation of Supersaturated Steam," Proc. Inst. of Mech. Engineers, Vol. III, Wet Steam 3, 184, part 3G (III), Paper 10, 22.

Pouring, A.A., "Effects of Heterogeneous Nucleation of Water Vapor in Nozzles," Trans. ASME 92, Ser D, 689 (J. Basic Eng.)

Stein, G.D., "Laserlichtstreuung an Zweiphasenströmungen," LASER und angewandte Strahlentechnik, Nr. 3.

Tkalenko, R.A., "O Spontanoi Kondensazyy Pry Obtekanyy Sverchsvylouym Potokom Vypuklogo Ugla," Mechanika Zhydkosti i Gasa, No.5, 73.

Varwig, R.L. and Mason, S.B., "Condensation in a Contoured Nozzle Shock Tunnel," AIAA J., 8, 1900.

Wegener, P.P. and Parlange, J.-Y., "Condensation by Homogeneous Nucleation in the Vapor Phase," Die Naturwissenschaften, 57, 525.

1971

Barschdorff, D., "Verlauf der Zustandsgrößen und gasdynamische Zusammenhänge bei der spontanen Kondensation reinen Wasserdampfes in Lavaldüsen," Forschung Ing.-Wes. 37, 146.

Clumpner, J.A., "Light Scattering from Ethyl Alcohol Droplets formed by Homogeneous Nucleation," J. Chem. Phys. 55, 5042.

1971 - continued

Homer, J.B., Hurle, I.R. and Swain, P.J., "Shock-tube Study of the Nucleation of Lead Vapor," *Nature*, 229, 251.

McBride, D.D. and Sherman, P.M., "Pitot Pressure in Hypersonic Flow with Condensation," *AIAA J.*, 9, 2354.

Pchelkin, I.M. and Alad'yev, I.T., "Investigation of the Expansion of a Water-Air Mixture in a Laval Nozzle," *Heat-Transfer-Soviet Research* 3, No.4, 34.

Pierce, T., Sherman, P.M. and McBride, D.D., "Condensation of Argon in a Supersonic Stream," *Astronautica Acta*, 16, 1.

Smith, L.T., "Experimental Investigation of the Expansion of Moist Air Around a Sharp Corner," *AIAA J.* 9, 2035.

Stollery, J.L., Gaydon, A.G., and Owen, P.R. (Editors) Shock Tube Research, Proceedings of the Eighth International Shock Tube Symposium, 5-8 July, Imperial College, London. Published by Chapman and Hall, London. See contributions by R.T.V. Kung and S.H. Bauer, "Nucleation Rate in Fe Vapor: Condensation to Liquid in Shock Tube Flow," paper 61; and by J.B. Homer, "Studies on the Nucleation and Growth of Metallic Particles from Supersaturated Vapours," paper 62.

1972

Barschdorff, D., Dunning, W.J., Wegener, P.P., and Wu, B.J.C., "Homogeneous Nucleation in Steam Nozzle Condensation," *Nature-Physical Science* 240, 166.

Davydov, L.M., "Study of Nonequilibrium Condensation in Supersonic Nozzles and Jets," *Fluid Mechanics, Soviet Research* 1, No.1, 90.

1972 - continued

Homer, J.B., and Hurle, I.R., "Shock-tube Studies on the Decomposition of Tetramethyl-lead and the Formation of Lead Oxide Particles," Proc. R. Soc. London A. 327, 61.

Kiang, C.S. and Mohnen, V.A., (Editors) International Workshop on Nucleation Theory and Its Applications, 10-12 April, Clark College, Atlanta, Georgia. See contributions by P.P. Wegener, "Introduction to Session V (Experimental Methods)" pp. 119 and 120; by B.J.C. Wu, "Status Report of Work at Yale University I. Nucleation Rates of Various Substances," p.121; by D. Barschdorff, "II. Homogeneous Nucleation in Steam," p.124; and by K.C. Russell, "Condensation of Vapors in Nozzles," p.132.

McBride, D.D. and Sherman, P.M., "Condensed Zinc Particle Size Determined by a Time Discrete Sampling Apparatus," AIAA J. 10, 1058.

Stein, G.D. and Moses, C.A., "Rayleigh Scattering Experiments on the Formation and Growth of Water Clusters Nucleated from Vapor Phase," J. Coll. Interface Sci., 39, 504.

Wegener, P.P., Clumpner, J.A. and Wu, B.J.C., "Homogeneous Nucleation and Growth of Ethanol Drops in Supersonic Flow," Phys. Fluids 15, 1869.

Wu, B.J.C., "A Study on Vapor Condensation by Homogeneous Nucleation in Nozzles," Doctoral Dissertation, Yale Univ., New Haven, Conn.

1973

Campbell, B.A. and Bakhtar, F., "Condensation Phenomena in High-Speed Flow of Steam-Experimental Apparatus," Heat and Fluid Flow (The Journal of the Thermodynamics and Fluid Mechanics Group of the Institution of Mechanical Engineers Proc. 187, 13/73). 3, No.1, 51. See also formal discussion on this paper by Wegener, P.P., in the same volume.

1973 - continued

Graham, S.C. and Homer, J.B., "Light Scattering Measurements on Aerosols in a Shock Tube," in Recent Developments in Shock Tube Research, Proceedings of the 9th International Shock Tube Symposium, Stanford Univ. 1973, Edited by D. Bershader and W. Griffith, Stanford Univ. Press.

Gyarmathy, G., Burkhard, H-P., Lesch, F. and Siegenthaler, A., "Spontaneous Condensation of Steam at High Pressure: First Experimental Results," Instn. Mech. Engrs., Conference Publication 3.

Kaser, A., "Verhalten von Dämpfen löslicher Zweistoffgemische bei Expansion in Überschalldüsen - Tropfenkoaleszenz in einer Potentialwirbelströmung," ZAMM 53, 39.

Kawada, H. and Mori, Y., "A Shock Tube Study on Condensation Kinetics," Bull. JSME 16, 1053.

1974

Barschdorff, D., Hausmann, G. and Ludwig, A., "Flow and Drop Size Investigations of Wet Steam at Sub- and Supersonic Velocities with the Theory of Homogeneous Condensation," Proceedings: Conference on Steam Turbines of Great Output, Polish Academy of Sciences, Institute of Fluid Flow Machinery, Gdansk, Poland.

Sislian, J.P., Kalra, S.P. and Glass, I.I., "The Non-equilibrium Condensation in a Mixture of Water Vapor/Carrier Gas in a Shock Tube," (ABSTRACT), Bull. APS II-19, 1150.

Wegener, P.P., "Condensation by Homogeneous Nucleation in Shock Tubes," Abstract for Conference EUROMECH 47, Univ. Southampton, England.

1974 - continued

Wegener, P.P., "Homogeneous Nucleation: Properties of Small Clusters," (ABSTRACT) Bull. APS II-19, 1150.

Wu, B.J.C. and Belle, K.C., "Condensation of Binary Vapors in a Shock Tube," (ABSTRACT) Bull. APS II-19, 1150.

Wu, B.J.C., "Computer Programs for Calculating Condensation Rate in Steady, Adiabatic Expansions in Supersonic Nozzles," Report 26 for Contract N00014-67-A-00197-0012. Available from National Technical Information Service, Springfield, Va., Ref. no. AD-775257.

1975

Barschdorff, D., "Carrier Gas Effects on Homogeneous Nucleation of Water Vapor in a Shock Tube," Phys. of Fluids, 18, 529.

Kalra, S.P., "Experiments on Nonequilibrium, Nonstationary Expansion of Water Vapour/Carrier Gas Mixtures in a Shock Tube," Report No.195, Univ. Toronto, Institute for Aerospace Studies, Toronto, Canada.

Puzyrewski, R., "Gasdynamic Effect of Condensation at High Pressure in Laval Nozzle," Archives of Mechanics, 27, 1, pp. 3-13, Warszawa, Poland.

Sherman, P.M., "Measurements of Submicron Fog Particles Generated in a Nozzle," J. Aerosol Science, 6, 57.

Wegener, P.P., "Nonequilibrium Flow with Condensation," Acta Mechanica, 21, 65.

Wegener, P.P., "Condensation by Homogeneous Nucleation Theory and Experiment," Invited paper. XII Biennial Fluid Dynamics Symposium. Advanced Problems and Methods in Fluid Dynamics. Proc. Pol. Ac. Sci. (in press).

TABLE CAPTIONS

- 4.1 Legend for Fig. 4.4. Collection of onset pressures and temperatures for condensation of water vapor in steady supersonic nozzle flow.
- 6.1 Number of water and ethanol molecules respectively in spherical drops of a given radius computed with Eqs. (5.22) and (5.23). Density for H_2O and CH_3-CH_2-OH condensate, 1 and 0.86 g/cm^3 , respectively, $T = 210 \text{ K}$.
- 6.2 Comparison of condensation results in nozzle and shock tube flow with nucleation theory. Data given pertain to the state at the onset of condensation and the supply of pure vapors (steam and N_2). (For theoretical expressions used note Sections 5 and 6.)
- 6.3 Comparison of condensation results of vapors in inert carrier gases in steady nozzle flow and shock tube experiments with nucleation theory. Data given pertain to the state at the onset of condensation and the supply. (For theoretical expressions used note Sections 5 and 6.)

FIGURE CAPTIONS

- 1.1 Schlieren picture of a "condensation shock" in a supersonic nozzle operated with moist air. This picture taken by A. Busemann and shown at the Volta Congress in Rome by Prandtl (1935) is believed to be the first published photographic record of condensation in supersonic flow. The "Mach lines" emanating from the walls are caused by the purposely roughened nozzle surface.
- 1.2 Schematic p-T diagram with coexistence line and isentrope. The adiabatic supercooling, ΔT_{ad} , and the critical supersaturation, p_{vk}/p_{∞} are defined.
- 1.3 Adiabatic supercooling of water vapor in air as a function of relative humidity in the atmospheric supply of a $(40 \times 40) \text{cm}^2$ supersonic wind tunnel in steady flow. Data obtained from Schlieren photographs (Eber and Gruenewald, 1941/42) with a $M = 1.86$ nozzle at a cooling rate of $\approx 10^5 \text{ C/sec}$.
- 1.4 Adiabatic supercooling of water vapor in air as a function of cooling rate in a steady Prandtl-Meyer expansion occurring in supersonic flow around a sharp 40° corner, for $41 < \phi_0 < 69\%$ (Smith 1971). The solid line shows an interpolation of the results with the limit for $dT/dt = 0$.
- 2.1 Area ratio and dimensionless flow properties as a function of Mach number in steady, inviscid nozzle flow with $\gamma \equiv c_p/c_v = 7/5 = 1.4$ (e.g. air).
- 2.2 Schematic diagram of the ideal operation of a shock tube. At top a time-distance plot. At time, t_1 , the instantaneous pressure and temperature is shown below with the corresponding flow features in the tube given at the bottom.

- 4.1 Experimental pressure distribution in two nozzles as a function of distance in steady nozzle flow from an atmospheric reservoir or supply with and without condensation (Wegener and Pouring 1964). (a) $\phi_0 = 29\%$, $dT/dt = -0.7 \text{ C}/\mu\text{sec}$. (b) $\phi_0 = 34\%$, $dT/dt = -2.8 \text{ C}/\mu\text{sec}$. The symbol indicates the results of a new complete solution of the equations of motion together with nucleation rate and droplet growth with $\log_{10} \Gamma = 4.7$ and $\alpha = 0.6$ (see Sections 5 and 6).
- 4.2 Flow parameters computed from the diabatic equations of motion through a heat addition zone caused by condensation of water vapor in air in a steady nozzle flow in a $(18 \times 18) \text{ cm}^2$ nozzle for $M = 2.92$ (Wegener 1954). Pressure distributions were measured for dry air and an atmospheric supply with $\phi_0 = 53\%$. T_{01} and p_{01} are supply temperatures and pressure with T_0 and p_0 being local values, respectively. Experimental onset of condensation is observed at $x = 1.6 \text{ cm}$.
- 4.3 Mean water cluster size and concentration as a function of initial specific humidity (H_2O mass fraction) computed from light scattering measurements assuming a delta-function size distribution as computed from Eqs. (4.1) and (4.2) (Stein 1969a). Steady supersonic flow, atmospheric supply of moist air, thermodynamic equilibrium at the observation station downstream from the condensation zone.
- 4.4 Pressure and temperature at the onset of water condensation (or critical supersaturation) in expansions of steam and moist air in steady supersonic nozzle flow. Different initial states and cooling rates are shown as identified in the references listed in Table 4.1 giving the symbols of this figure.
- 5.1 Schematic of symbols and states used in droplet growth calculations.

- 6.1 Observed (shaded area) and computed (solid line) mass fraction of liquid ethanol in air in steady supersonic nozzle flow (Wegener et al. 1972). The shaded area indicates the experimental uncertainty. Nucleation rate, number density of clusters and saturation ratio as computed for this experiment with an atmospheric supply and $\omega_0 = 0.005$. Note distance and area scales. Time scale computed with Eq. (2.32). In the calculations with nucleation rate and growth, $\Gamma = 10^5$, $\alpha = 0.7$ and $\sigma \equiv \sigma_\infty$, see Section 5.
- 6.2 Critical radius and selected droplet radii in steady nozzle flow for liquid ethanol as computed from Volmer's Eq. (5.20) with $\sigma/\sigma_\infty = 0.725$ for the experimental environment described in Fig. 6.1. Normalized drop size distribution at the nozzle exit is shown on the right.
- 6.3 Experimentally observed critical supersaturation as a function of temperature for steam condensation in steady supersonic nozzle flow and a shock tube. The solid line shown is derived from all supersonic nozzle steam experiments listed in Table 4.1. Temperature made dimensionless by $T_{\text{crit}} = 647$ K.
- 6.4 Ratio of observed and computed nucleation rates (non-isothermal theory, Eqs.(5.20) and (5.28) at the onset of condensation as a function of initial specific humidity obtained in the expansion fan of a shock tube (Barschdorff 1975). Note different carrier gases: \diamond air, \square helium, \circ argon, \triangle none (steam).
- 6.5 Ratio of observed and computed nucleation rate at the onset of condensation of steam in supersonic nozzle flow (Barschdorff et al. 1972). Results from non-isothermal

nucleation theory, Eqs. (5.20) and (5.28)——, and isothermal theory Eq. (5.20) ---, are given as a function of condensation coefficient for a single experimental result for $p/p_\infty = 8.1$ (Barschdorff 1971), cf. line 3, Table 6.2.

- 6.6 Critical supersaturation as a function of temperature of water vapor present in small concentrations in carrier gases. Temperature function according to Eq. (6.4). Results from cloud chambers, nozzles and shock tubes are shown.
- 6.7 Critical supersaturation of steam from nozzle and shock tube experiments plotted as in Fig. 6.6.
- 6.8 Matched values of the surface tension and the replacement factor, Eq. (5.20) compatible with experiments on the onset of condensation of ethanol in air ($\omega_0 = 0.005$) for the experiment described in Fig. 6.1 (Wegener et al. 1972). Error bar indicates the uncertainty in the measured nucleation rate.
- 6.9 Numerical values for the terms entering the nucleation rate Eqs. (5.20, (5.25), and (5.26) in steady nozzle flow of ethanol ($\omega_0 = 0.005$) in air of the experiment described in Fig. 6.1 (Wegener et al. 1972). Independent calculations of the replacement factor in the expression of Eq. (5.26) for Γ , following the models of Lothe and Pound (1966) and Dunning (1965) respectively. Computed experimental value of Γ , based on Eq. (6.1), see also Table 6.3. Agreement of Γ_{exp} and Γ_{D} implies that the classical nucleation rate, e.g. Eq. (5.20) gives results remarkably close to the experiment at the onset of condensation.

TABLE 6.1

$r(\text{\AA})$	n_{water}	n_{ethanol}
4	9	3
6	30	10
8	72	25
10	140	47
12	242	81

TABLE 4.1

Symbol	Author (year)	Cooling Rate (C/ μ sec)
◇	Binnie & Green (1943)	1
△	Pouring (1963)	0.7 and 3
□	Gyarmathy & Meyer (1965)	1 and 0.3
×	Stein (1967)	2
‡	Deych, Stepanchuk & Saltanov (1969)	2
▼	Roberts (1969)	1
●	Barschdorff (1971) and Barschdorff & Ludwieg (1972)	0.6
+	Stein & Moses (1972)	1